Summer 2024

Advanced Mass Spectrometry Method Development and Applications for Assessment of Traumatic Brain Injury and Legionella Pneumophila Dissinfection with Copper

Austin Chase Sigler
Missouri University of Science and Technology

Department: Chemistry

ADVANCED MASS SPECTROMETRY METHOD DEVELOPMENT AND APPLICATIONS FOR ASSESSMENT OF TRAUMATIC BRAIN INJURY AND LEGIONELLA PNEUMOPHILIA DISINFECTION WITH COPPER

by

AUSTIN CHASE SIGLER

A DISSERTATION

Presented to the Graduate Faculty of the

MISSOURI UNIVERSITY OF SCIENCE AND TECHNOLOGY

In Partial Fulfillment of the Requirements for the Degree

DOCTOR OF PHILOSOPHY

in

CHEMISTRY

2023

Approved by:

Honglan Shi, Advisor
Paul Nam, Co-Advisor
Casey Burton, Co-Advisor
Risheng Wang
David Westenburg

PUBLICATION DISSERTATION OPTION

This dissertation consists of one peer-reviewed article published elsewhere, one submitted for review to a publication, and one intended for submission to another journal. These are formatted in the style used by the Missouri University of Science and Technology in addition to an original introduction and conclusion:

Paper I, found on pages 9-33, has been published by Journal of the American Society for Mass Spectrometry 31(9):1910-1917 (2020).

Paper II, found on pages 34-56, has been submitted for review to Metabolites.

Paper III, found on pages 57-89, is intended for submission to Analytical and Bioanalytical Chemistry.

ABSTRACT

Pathological processes often involve complex biochemical changes which can be assessed using advanced mass spectrometry. In this present dissertation, two fields were studied: traumatic brain injury (TBI), and water contamination by L. pneumophilia. TBI is a pressing public health concern for which current clinical tools remain inadequate. We present newly developed mass spectrometric methods to access metabolites associated with blast induced TBI. We applied these methods to the biofluids of soldiers conducting explosives training. Significant changes in several metabolites were observed between pre- and post-blast specimens, including changes that increased with repeated exposure. These changes point to the possibility of a biomarker panel to assess the severity of blast related TBI. L. pneumophilia is a pathogenic bacteria which can infect domestic water supplies. Its control and prevention in these systems is of major public health consequence. We have developed a novel single cell-inductively coupled plasma- mass spectrometry (SC-ICP-MS) method and applied this method to investigate L. pneumophilia treatment efficiency by copper (Cu) in drinking water. We applied this method to L. pneumophilia dosed with Cu in varied concentrations and over a time. Interestingly, high concentrations of Cu ions were found to have a high disinfection rate in drinking water, some cells persisted and even returned to a normal state 24 hours after the initial exposure to Cu. These likely viable but non-culturable cells were detectable by SC-ICP-MS but not by colony forming unit count analyses. This is the first study to our knowledge which explores the relationship between copper dosing over time of L. pneumophilia in drinking water by SC-ICP-MS.

ACKNOWLEDGMENTS

I could have never made it to this point in my career without the support of a team of talented individuals collectively pushing me forward to success. Firstly, I want to thank my research advisor Dr. Honglan Shi, for having significant patience with me as a grew into a better researcher and also believing that I could accomplish worthwhile goals even when I did not believe that myself. Thanks also to my co-advisors Dr. Casey Burton and Dr. Paul Nam. Dr. Burton introduced me to the interface between clinical research and basic scientific discovery, and cleared many administrative and technical hurdles so that my work could be possible. Dr. Nam not only taught me the basic scientific principals I needed to know, but also how to apply and translate those into meaningful research experiments. Thanks to my additional committee members Dr. Rishing Wang and Dr. David Westenburg for their valuable insights and critical analyses which helped to hone this work. Thank you to the research teams of Drs. Shi and Nam, as well as Lei Xu, Anna Chernatskya, and Dr. Jiandong Wu for valuable mentorship, helping design experiments and edit manuscripts, and providing companionship throughout my program. Finally, I would like to thank all of my family and friends who supported me throughout this journey. Thanks to Mr. Brett Parker and Mr. Thomas Miller, for always having a listening ear when times got tough. Thanks to my mother, who always believed in me even when I had doubts. Lastly, thanks to my wife, for her constant love and support.

TABLE OF CONTENTS

PAPER

SECTION

LIST OF ILLUSTRATIONS

LIST OF TABLES

1. INTRODUCTION

1.1. PUBLIC HEALTH AND CHEMICAL BIOMARKERS

From the beginning of civilized society, public health concerns have been an active area of research interest. From centuries old sanitation practices developed to reduce disease outbreaks, to innovative precision medicine aimed at assessing and mitigating genetic risk factors for chronic conditions, some of the greatest accomplishments history can boast of are rooted deeply in the detection and prevention of disease. Given our rapidly expanding global population, new assessment techniques for disease, many of which are rooted in molecular biomarkers, could be key in facing emerging public health challenges [1]. Mass spectrometry offers significant advantages as a platform for both discovery of new potential clinical biomarkers [2], and validating those biomarkers in disease states [3]. Indeed, multiple pathophysiological processes including coronary artery disease [4], cancer [5]–[7], and even neurodegenerative diseases [8], [9] all have biomarkers which have been studied by various mass spectrometric techniques. The role of mass spectrometry in "omics" based profiling and characterization is expected to expand considerably due to advances in data analysis tools and mass spectrometric sensitivity [10].

However, despite these advancements, some pathological processes of public health concern have remained elusive. Traumatic brain injury (TBI) involves a complex neurochemical cascade of events, some of which can alter based on the type and location of the insult, the history of prior TBI events, and other confounding factors. Legionella bacteria are difficult to study due to their unique biphasic lifestyle and presence of viable

but non-culturable cell morphologies. Understanding the processes by which these public health concerns emerge requires judicious selection of molecular and chemical targets, and powerful analytical techniques to probe those processes.

1.2. TRAUMATIC BRAIN INJURY

Traumatic brain injury accounts for several million emergency room visits, hospitalizations, and deaths every year in the United States [11]. In addition to the severe acute damage TBIs cause, victims often suffer significant long-term effects including neural deficits [12], post-traumatic stress disorder (PTSD) [13], Alzheimer's disease [14], [15], and others[16], [17]. The complex nature of TBI also makes it difficult to predict long term clinical outcomes, and unfortunately strong evidence to support treatment guidelines and recommendations is unacceptably scarce [18]. Much has been learned in recent years regarding both the pathophysiological mechanisms associated with TBI and biomarkers to assess overall severity [19]–[22]. Some of the most widely studied TBI biomarkers are proteins which measure specific molecular events. Ubiquitin C-terminal hydrolase-L1 (UCH-L1) [23], [24], glial fibrillary acidic protein (GFAP) [25], [26], S100β [27], and other proteins have all been implicated in predicting TBI severity or outcomes in clinical settings. However, despite this progress, a reliable clinical assessment tool capable of prognosing long term clinical outcomes has yet to be achieved. In addition, little is known about the mechanisms which govern the transition from the initial insult to long term outcomes, especially when the initial insult is mild.

Monitoring neurochemical and metabolomic changes in TBI, via molecular biomarkers in biofluids, could provide increased understanding of TBI and its prognostic outcomes.

1.2.1. Metabolic Pathways Implicated in TBI. Several metabolic pathways and processes are involved in TBI pathophysiology. While an in depth review of all of these is beyond the scope of this dissertation, a brief overview of some key pathways is warranted.

1.2.1.1. Altered neurotransmission. Following the initial insult of a TBI, elastic deformation of nerve cells leads to disruption of cellular membranes. Intracellular potassium release into the extracellular fluid causes indiscriminate neurotransmitter release [28]. Excitatory neurotransmitters such as dopamine and glutamate can be severely dysregulated as a result of this indiscriminate release [29]–[31]. Both dopaminergic and glutamatergic metabolic pathways have also been implicated in cognitive impairment following TBI in rodent models [31], [32]. This altered neurotransmission is a major complicating factor in TBI which can lead to further dysfunction and long term clinical consequences.

1.2.1.2. Oxidative stress. While many pathophysiological processes can lead to or result from oxidative stress and it should not be considered brain specific, it is important to note the role it plays in TBI. Oxidative stress in TBI results from the secondary injury following the initial insult. Excitotoxicity, release of neuronal intracellular components, and response to cell death can activate body responses to restore homeostasis and increase reactive oxygen species (ROS) systemically [33]. One novel therapeutic method even attempts to treat TBI by mitigating the oxidative stress at

the endothelial level [34]. Several markers of oxidative stress have been monitored previously in TBI [35], [36].

1.2.1.3. Metabolic changes. While much research focuses on the acute phase, from initial impact to several hours or days post-injury, significant metabolic changes can also occur in the chronic phase of TBI, and those changes can result in cognitive decline and dysfunction [37]. Specifically, changes in lipid metabolism and lipid peroxidation can affect important functional components of neural cells and alter function significantly[38], [39]. Changes in glucose metabolism and glycolysis have also been observed in TBI, indicating the importance of respiration products following injury [40], [41].

1.2.2. Biofluids for TBI Characterization. Cerebrospinal fluid (CSF) has long been regarded as a gold standard for brain injury assessment. Given its direct interface with the extracellular matrix of the brain, and insulation from confounding extracerebral factors which may influence biomarker levels, it is considered ideal for assessing biochemical changes in brain injuries [42]. However, collecting CSF is invasive, and may not yield large enough volumes for analysis, particularly in penetrating injuries. CSF is also a complicated matrix for analytical methods, and may require extensive sample preparation and cleaning and/or pre-concentration techniques prior to analysis. Serum has also been widely used, but suffers from many of the same problems as CSF [43]. While collection of serum is not as invasive as CSF, low sample volumes can confound analyses and complex sample matrix can add several steps to analysis procedures. Urine, by contrast, is a relatively simple matrix with few interfering lipids or proteins [44], [45]. Urine is also easy to collect in large volumes, and is a promising biofluid for non-

invasive TBI biomarker characterization [45], [46]. Additionally, some of the same biomolecules which have already been studied in serum or CSF as potential TBI biomarkers can also be monitored in the urinary matrix [46]–[48].

An additional factor to consider when assessing the feasibility of a biofluid for this purpose is the sensitivity of the changes occurring. The ideal biofluid biomarker for TBI should be highly brain specific, accurate, and have a rapid change following TBI [49]. The ideal biomarker should also provide clinical value, adding diagnostic or prognostic information not already available from clinical evaluation [49]. These biomarker qualifications are particularly difficult to achieve in mild TBI. However, growing evidence suggests that even subconcussive events, when repeated, can lead to more severe long term clinical consequences [50]–[52].

1.2.3. Special Considerations for Repeated and Blast TBI. Blast induced TBI (bTBI) is a subset of TBI which, as opposed to a blunt force insult, results from the indirect exposure to blast overpressures. Millitary personel encounter explosive blasts frequently during training and combat operations [53], [54]. Such repeated exposures are infrequent in blunt force related TBI, and the repeated exposures have been shown to have cumulative effects in both human studies and rodent models [12], [50], [55]–[58]. These cumulative effects, while not well understood, may indicate an increased suceptability to TBI, and thus increased hazard, for people who have had prior exposures. Modeling of blast related injuries, and particularly those which are low level yet repeatative, has also been a challenge for researchers in this field.

While widely accepted clinical models of TBI such as controlled cortical impact (CCI) [59], can provide valuable insights into blunt force TBI, they are inadequate to

assess bTBI in the same way. Fluid percussion modeling does a somewhat better job at reproducing elastic deformation and other clinical hallmarks of TBI [60], but there has been some discussion that an open field blast model may be superior in bTBI studies [58], [61].

1.3. LEGIONAIRE'S DISEASE

Legionella pneumophila (*L. pneumophila*) is a persistent opportunistic pathogen which can cause a serious form of pneumonia called Legionnaire's disease (LD). While several Legionella bacteria are capable of causing LD, L. pneumophila is responsible for >90% of all LD cases [62], [63]. Due to the routes by which L. pneumophilia may spread, through domestic water systems [64], [65], building cooling towers [66], or others [67], [68], and the severity of the disease, early clinical management and prevention of outbreaks are vital to public health, particularly in population dense areas [63], [69]. Several methods to treat water systems to eliminate or prevent these bacterial threats exist and are detailed below.

1.3.1. Water Treatment Methods. Supplying a population with drinking water free from *L. pneumophilia* contamination represents one of the most significant public health challenges to date. While efficacy of the disinfection method is often of greatest concern, weight also must be given to competing factors such as formation of harmful disinfection byproducts (DBPs) [70]. Chlorination, for example, is a ubiquitous water disinfection solution due to its effectiveness and relative ease of implementation [71], [72]. However, several problems can arise from chlorination of water, including unfavorable taste and odor [73], [74], ineffectiveness against resistant microorganisms

[75]–[77], and formation of harmful disinfection byproducts [71], [78], [79]. Other oxidative disinfection methods such as ozonation or even electrochemical oxidation have also been studied both alone and in combination with chlorination [80]–[82], but suffer from similar, albeit distinct DBP formation challenges [83]. These formations can be reduced considerably through studying the mechanisms by which they form, but are unlikely to ever fully resolve [84]. Some metal ion and nanoparticle-based disinfection methods [85]–[87], have been studied as attractive options to reduce or eliminate the risk from DBPs. However, the efficacy of these methods on microorganisms, and the long-term consequences of their implication, are still under investigation [88]. Despite these treatment methods, *L. pneumophilia* remains notoriously resilient and often confounds current treatment methods [77], [89]–[91]. Some of the mechanisms by which L. pneumophila manages such resistance are detailed below.

1.3.2. Mechanisms of Treatment Resistance *L. pneumophilia* is a resilient and highly adaptive pathogen that can endure a wide range of temeratures, relatively high salinity, and even resist digestion from host amoeba and propagate in human lung macrophages [92]. Legionella are known to form resistant biofilms [93], [94], which, if disrupted, can introduce large doses of the pathogen into domestic water systems [95]. Since legionella can also reproduce within amoeba, aresolization of a single amoeba can introduce an infectious dose of bacteria into human hosts [96]. These adaptations certainly contribute to L. pneumophilia persistence in domestic water systems. Additionally, one of the most interesting adaptations L. pneumophilia exhibits is the ability to form viable but non-culturable (VBNC) cells which can persist in disinfection and return to a culturable state following disinfection [90], [91]. Such VBNC cells are

highly resistant to treatment methods, but the details of their formation and how they persist in hostile environments is not yet well understood. An advanced analytical methods to monitor cells in suspension may be key in understanding how this biological process proceeds.

1.3.3. SC-ICP-MS to monitor L. Pneumophilia Single cell inductively coupled plasma mass spectrometry (SC-ICP-MS) is an emerging analytical technique used to study metal content in populations of cells. With this technique, researchers can determine many important biological parameters of their cell population including cell concentration, intrinsic or dosed metal concentration per cell, and quantitative uptake of metal ions or even nanoparticles by those cells [97]. This application has already been applied to a number of cell types, including yeast [98], S. areus and E. coli [99], alge [100], human erythrocytes [101] and human cancer cells[102]. Using SC-ICP-MS to monitor L. pneumophilia and its response to treatment conditions could give insight into how the resistance develops and potentially how to more effectively disinfect water systems contaminated with the opportunistic pathogen.

PAPER

I. SIMULTANEOUS DETERMINATION OF EIGHT URINARY METABOLITES BY HPLC-MS/MS FOR NONINVASIVE ASSESSMENT OF TRAUMATIC BRAIN INJURY

Austin Sigler,1 Xiaolong He,1 Mousumi Bose,1 Alexandre Cristea,1 Wenyan Liu,1 Paul Ki-souk Nam,1 Donald James,2 Casey Burton,1,2* and Honglan Shi1*

1Deparment of Chemistry, Missouri University of Science and Technology, Rolla, MO, 65409

2Phelps Health, Rolla MO, 65409

Correspondance:

Casey Burton - Department of Chemistry, Missouri University of Science and Technology, Rolla, Missouri 65409, United States; Phelps Health, Rolla, Missouri 65401, United States; Orcid: http://orcid.org/0000-0002-0729-6743; Email: c.f.burton@mst.edu

Honglan Shi - Department of Chemistry, Missouri University of Science and Technology, Rolla, Missouri 65409, United States; Orcid: http://orcid.org/0000-0002-0801-5683; Email: honglan@mst.edu

ABSTRACT

Traumatic brain injury (TBI) is a serious public health concern for which sensitive and objective diagnostic methods remain lacking. While advances in neuroimaging have improved diagnostic capabilities, the complementary use of molecular biomarkers can provide clinicians with additional insight into the nature and severity of TBI. In this study, a panel of eight metabolites involved in distinct pathophysiological processes related to concussion was quantified using high-performance liquid chromatography-tandem mass spectrometry (HPLC-MS/ MS). Specifically, the newly developed method

can simultaneously determine urinary concentrations of glutamic acid, homovanillic acid, 5-hydroxyindoleacetic acid, methionine sulfoxide, lactic acid, pyruvic acid, N-acetylaspartic acid, and F2α-isoprostane without intensive sample preparation or preconcentration. The method was systematically validated to assess sensitivity (method detection limits: 1−20 μg/L), accuracy (81−124% spike recoveries in urine), and reproducibility (relative standard deviation: 4−12%). The method was ultimately applied to a small cohort of urine specimens obtained from healthy college student volunteers. The method presented here provides a new technique to facilitate future work aiming to assess the clinical efficacy of these putative biomarkers for noninvasive assessment of TBI.

Key words: traumatic brain injury (TBI), biomarkers, HPLC-MS/MS, urine analysis, non-invasive assessment

1. INTRODUCTION

Traumatic brain injury (TBI) is a significant public health concern that accounts for several million emergency room visits, hospitalizations, and deaths every year in the United States.1 This challenge is compounded by the various long-term clinical outcomes that can accompany survivors, including post-traumatic stress disorder (PTSD), Alzheimer's, and other dementias, among other mental and cognitive health conditions. The ability to objectively diagnose and characterize traumatic brain injury therefore continues to be a clinical research priority. Currently, concussive injuries are evaluated by an assortment of neurological assessments, including neuropsychological evaluations,

acute injury surveillance, and medical imaging. Among the most widely employed assessments are the Military Acute Concussion Exam (MACE), Glasgow Coma Scale (GCS), and evaluations of duration of loss of consciousness (LOC) and post traumatic amnesia (PTA). These methods are useful for rapid assessments of severe head trauma, but have limited diagnostic value for mild TBI given the relatively limited time frame for acute symptom manifestation2−4 and their assessment of outcomes that are not exclusively associated with concussive injury.5 Neuroimaging, including computed tomography (CT) and magnetic resonance imaging (MRI), can be used to detect a multitude of structural abnormalities in brain tissue, rendering them powerful tools in assessing moderate and severe TBI. However, many traumatic brain injuries can appear relatively normal under conventional CT and MRI scans.6,7 Recent advances in neuroimaging techniques, such as diffusion tensor imaging, have allowed researchers to detect subclinical changes in brain structure, including diffuse axonal injury.6,8 While these advanced neuroimaging tools can help elucidate subtle structural changes associated with persistent postconcussive symptoms,3,6−8 the implementation of diagnostic imaging for field assessments remains limited by high costs and poor accessibility, particularly in rural and other remote areas. Molecular biomarkers can provide additional biological information about concussive injuries that can complement conventional neurological assessments and medical imaging. Prior efforts to identify TBI biomarkers have noticed novel associations between several proteins found in cerebrospinal fluid (CSF) and serum to clinical outcomes in patients with TBI.9 For example, glial S100β, which is involved in low affinity calcium binding in astrocytes, has been connected to astrocyte stress and death.10 Glial fibrillary acidic protein (GFAP) has

also been extensively studied owing to its function as an intermediate filament protein in astrocytes, where increased serum levels have been associated with astrocyte damage.11,12 Additionally, serum levels of neuronal, specifically axonal, damage indicators, including neuron-specific enolase,13 cleaved tau protein,14 and ubiquitin C-terminal hydrolase,15,16 have been correlated with poor clinical outcomes. Improved understanding of the pathophysiology underlying traumatic brain injuries has further prompted interest in studying the complex metabolic cascade that is a key characteristic of TBI. Immediately following a concussive event, a disruption of cellular homeostasis and failure of cellular membrane integrity results in the release of K+ ions, resulting in axonal depolarization and the subsequent indiscriminate release of excitatory neurotransmitters.17,18 These neurotransmitters and their derivatives, including homovanillic acid (HVA),19 glutamate,20 and 5-hydroxyindoleacetic acid (5-HIAA),21 have each been the subject of investigations in traumatic brain injury. Specifically, an increase in cerebrospinal fluid (CSF) glutamate levels immediately following the K+ release has been noted in a previous study.20 It is further predicted that additional neurotransmitters and their derivatives play a significant role in the neurochemical cascade of concussion.17−21 Following the release of K+ ions, ATP-dependent Na+ and K+ pumps are activated to restore electrolytic balance in the brain, resulting in significant metabolic energy demands. For this reason, glucose metabolism, and in particular, the glycolytic intermediates lactate and pyruvate have been proposed as possible indicators of TBI progression and subsequent recovery.22 For example, the ratio of lactate to pyruvate has been suggested to indicate hyperglycolysis in TBI, and the ratio was found to increase before terminal brain herniation in severe TBI patients.17,22−24 Furthermore,

excess oxidative stress occurs as a result of mitochondrial damage and altered oxidative metabolism, which has prompted interest to explore oxidative stress metabolites, most notably N-acetylaspartic acid (NAA)25,26 and F2α-isoprostane,27,28 as potential TBI biomarkers. This complex pathophysiological cascade invokes distinct metabolic processes that may therefore be probed to assess the extent and nature of the injury.17,18,29 We have therefore proposed a novel combination of these interesting metabolites, shown in Figure 1, alongside several established protein biomarkers, to study potential patterns and differences in TBI samples. This panel, composed of a combination of excitatory neurotransmitters, glycolytic intermediates, and oxidative stress indicators, represents broad and diversified potential biomarkers of neurological processes involved in TBI. In particular, the development of a metabolic panel of potential biomarkers presents a novel advancement in the molecular detection of traumatic brain injury.

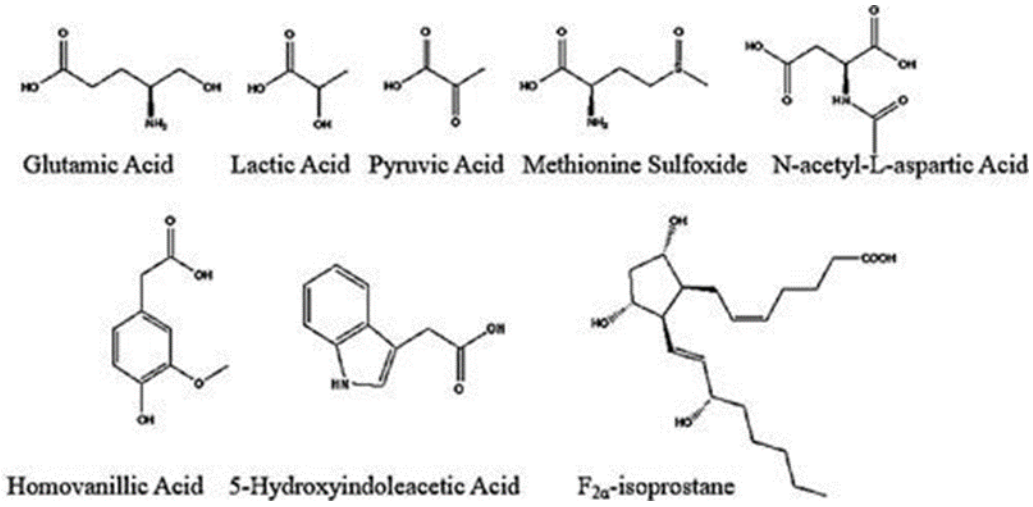

Figure 1. Chemical structures of the eight TBI-related metabolites.

While cerebrospinal fluid has conventionally served as the gold standard for brain metabolite quantitation, owing to its direct contact with the extracellular matrix of the brain,30 urine and serum present minimally invasive specimen types that can be readily obtained in the field. In particular, urine offers several advantages including large sample volumes, fewer sample pretreatment requirements, and noninvasive sample collection requiring no medical expertise. However, and to the best of our knowledge, a comprehensive panel of TBI biomarkers has yet to be developed in urine. While a limited number of such biomarkers have been successfully measured in urine,31−34 previous methods have focused primarily on individual biomarkers and have often involved intensive sample derivatization and extraction steps.33,35,36 In this study, we have therefore proposed a new technique for simultaneous determination of eight chemically diverse metabolites in urine without intensive sample preparation using high-performance liquid chromatography-tandem mass spectrometry (HPLC-MS/MS). This novel approach may provide timely supplemental characterization of traumatic brain injuries in the field, thereby presenting new opportunities for mitigating long-term outcomes in both civilian and military populations.

2. EXPERIMENTAL

2.1. MATERIALS

Analytical grade standards for homovanillic acid (HVA), glutamic acid (Glu), lactic acid (Lac), pyruvic acid (Pyr), methionine sulfoxide (MetSO), N-acetylaspartic acid (NAA), and isotopically labeled glutamic acid (13C, 15N) were purchased from

Sigma-Aldrich, (St. Louis, MO, USA). 5- Hydroxyindoleacetic acid (5-HIAA), LCMS-grade methanol, and acetonitrile (ACN) were purchased from Fischer Scientific (Hampton, NH, USA). F2α-Isoprostane was purchased from Cayman Chemicals (Ann Arbor, Michigan, USA). Ultrapure water (18.2 MΩ.cm) was generated in-house by a Millipore Elix-3 purification system (Millipore, Billerica, MA, USA).

2.2. STANDARD PREPARATION

Analytical standard stock solutions were prepared at 1000 mg/L in 90:10 ultrapure water/ACN with the exception of F2α-isoprostane, which was prepared in pure methanol according to manufacturer instructions. These stock standard solutions were stored at 4 °C, except for F2a-isoprostaglandin, which was stored at −20 °C. Secondary standard mixtures of the analytes were prepared by diluting stock solutions in ultrapure water and maintained at the same temperatures noted above. Calibration standard solutions were prepared by serial dilution of the secondary standard mixture in 9:1 ultrapure water/ACN and synthetic urine solution to simulate 200-fold diluted urine. Standards used for mass optimizations were prepared in mixtures of ACN and ultrapure water with 0.1% formic acid to facilitate optimum ionization under ESI conditions. Synthetic urine was prepared in-house by combining 3.75 g of sodium chloride, 2.25 g of potassium chloride, 2.4 g of monosodium phosphate, and 9.1 g of urea to 375 mL of ultrapure water. The resulting synthetic urine was vortexed thoroughly and stored at 4 °C for calibration blank and calibration standard preparation. The synthetic urine was reprepared monthly.

2.3. URINE SAMPLE PREPARATION

Urine samples from Missouri University of Science and Technology student volunteers without known ailments were obtained and stored at −80 °C until analysis. Samples were thawed at room temperature, and a 100 μL aliquot was diluted with 800 μL of methanol, 50 μL of ultrapure water, and 50 μL of internal standard solution consisting of 160 mg/L Glu (13C, 15N). Samples were subsequently vortexed, allowed to precipitate for 20 min at room temperature (~25 °C), and finally centrifuged for 20 min at 10000g. Following centrifugation, 50 μL of supernatant was diluted with 950 μL of 9:1 ultrapure water/ACN for a total urine dilution factor of 200-fold for HPLC-MS/MS analysis.

2.4. HPLC-MS/MS METHOD

A Shimadzu (Columbia, MD, USA) Prominence UFLC system consisting of a degasser (DGU-30A3), two pumps (LC-20 AD XR), an autosampler (SIL-20AC XR), and a column oven (CTO-20A) were coupled to a 4000 QTRAP tandem mass spectrometer system (AB SCIEX, Concord, ON, CA) and controlled by Analyst Software to separate and quantitate analytes in this study. A HydroRP column (4 μm, 150 × 2 mm) purchased from Phenomenex (Torrance, CA, USA) was employed for separation. HPLC was performed at 40 °C column temperature with binary flow at a rate of 0.3 mL/min with mobile phase A consisting of 0.1% formic acid in ultrapure water and mobile phase B consisting of 0.1% formic acid in ACN. The method began with a prerun equilibration of 4 min at 100% A and continued with 100% A after injection of 20 μL of sample for the initial 2 min, followed by a linear gradient increase to 100% B from 3 to 7 min and hold

at 100% B from 7 to 10 min, finally changed to 100% A from 10 to 10.5 min. The run-to-run time was 14.5 min. Negative electrospray ionization (ESI-) mode and multiple reaction monitoring (MRM) were optimized for quantification analysis. Curtain gas and collision gas were generated by a model Genius 1024 230 V nitrogen generator (Peak Scientific, Billerica, MA, USA). The ion source temperature was set to 550 °C. The ion spray voltage was set to −4500 V. The curtain gas was set to 25 psi, and the ion source gases (GS1 and GS2) were at 40 and 15 psi, respectively. All mass spectrometer conditions were optimized for quantitative detection of the analytes.

2.5. URINE SPECIFIC GRAVITY MEASUREMENTS

Hydration status and time since last urination causes changes in urine concentration dilution that must be corrected for accurate biomarker quantitation. Because creatinine-based corrections are influenced by a variety of demographic and clinical factors, urine specific gravity (USG) correction37 was used in this study to account for urine concentration dilution. USG was measured refractometrically using a Reichert digital Clinic Chek Digital Hand-held Refractometer. Urine specimens were equilibrated to room temperature before measurement by the refractometer. Ultrapure water was used as a quality control standard.

3. RESULTS AND DISCUSSION

3.1. MS/MS DETECTION OPTIMIZATION

The ionization efficiency of the eight metabolites were initially assessed in both positive- and negative-mode electrospray ionization (ESI) using a variety of additives. The carboxylic acid functionalities present on all eight metabolites facilitated excellent ionization under negative-mode ESI (ESI-). While ammonium salts, such as ammonium acetate, are routinely used in ESI- applications to promote deprotonation without significant cation adduction,38,39 addition of 1−10 mM ammonium acetate resulted in significant signal suppression for lactate, pyruvate, and glutamate. Meanwhile, 0.1% v/v formic acid was found to afford sufficient ionization for all species without noticeable ion suppression, although formic acid concentrations exceeding 0.2% v/v deteriorated peak shapes in several early eluting compounds. Therefore, mass optimizations were performed by direct infusion of standards using a syringe pump operating at 0.6 mL/h flow rate. Infusion standards were prepared by dilution of the primary standards with a solution of ultrapure water/ACN (9:1, v/v) with 0.1% (v/v) formic acid. Nitrogen gas was used for the collision and curtain gases. Precursor ions were scanned with a scan range from 100 m/z above the expected target molecular ion in order to monitor potential adduct ion formation. Initial Q1 scans of each analyte in broader mass ranges revealed no significant adduct ion formation. Once the precursor ion was identified, product ion scans were employed to elucidate major product ion formation. The two most abundant product ions were then optimized with respect to the declustering potential (DP), collision energy

(CE), and collision cell exit potential (CXP). The optimized parameters are listed in Table 1. All other parameters were optimized by flow injection.

3.2. CHROMATOGRAPHIC SEPARATION

Chromatographic separation was further used to minimize the potential for mass spectrometric interferences resulting from the multitude of urinary metabolites present in the selected mass range. Both FusionRP (150 × 2 mm) and HydoRP (150 × 2 mm) columns were evaluated. The FusionRP column phase includes a polar embedded group on a C18 base structure, which allows for Hbond donating and accepting capabilities, giving this phase balanced selectivity across polar and nonpolar analytes.

The HydroRP column relies on a polar end-capped C18 phase, which allows for very high hydrophobic interactions while also facilitating H-bond donation and thus enhanced polar retention as compared with a typical C18 phase, though notably not as high polar retention as the FusionRP phase. Given the diverse chemical properties as well as sizes of the target compounds, the chemistries of these two columns showed potential to deliver a high quality separation. While the FusionRP column showed promising separations with excellent detection limits and short retention times of the analytes, the spike recoveries of some analytes were poor in real urine samples due to significant ion suppression from ionic salts and other components in the urine. The broader selectivity of the FusionRP column as compared to the HydroRP could have allowed for increased retention of undetected matrix components in urine which coeluted with the analytes and then caused ion suppression at the target transitions.

Table 1. Optimized MS/MS Parameters of the Eight Metabolites

Compound	**Abbreviation**	**Ion Pair Masses**	**DP (volts)**	**CE (volts)**	**CXP (volts)**
Methionine Sulfoxide (Q)	MeSO	164.1/63.2	-60	-18	-5
Methionine Sulfoxide (C)	MeSO	164.1/100.3	-60	-16	-7
Glutamic acid (Q)	Glu	146.0/102.3	-50	-18	-9
Glutamic acid (C)	Glu	146.0/128.3	-50	-16	-5
Lactic Acid (Q)	Lac	89.0/43.3	-45	-20	-5
Lactic Acid (C)	Lac	89.0/61.3	-45	-16	-5
Pyruvic Acid (Q)	Pyr	87.1/43.3	-35	-12	-5
Pyruvic Acid (C)	Pyr	87.1/44.3	-35	-12	-1
N-Acetylaspartic acid (Q)	NAA	174.2/88.3	-38	-21	-3
N-Acetylaspartic acid (C)	NAA	174.2/58.3	-41	-29	-8
Homovanillic acid (Q)	HVA	181.0/137.3	-48	-11	-7
Homovanillic acid (C)	HVA	181.0/122.2	-50	-21	-9
5-Hydroxyindoleacetic acid (Q)	5-HIAA	190.1/146.2	-50	-16	-7
5-Hydroxyindoleacetic acid (C)	5-HIAA	190.1/144.3	-50	-28	-7
$F_{2\alpha}$-Isoprostane (Q)	$F_{2\alpha}$	353.2/193.1	-95	-36	-11
$F_{2\alpha}$-Isoprostane (C)	$F_{2\alpha}$	353.2/309.2	-95	-28	-7
Glutamic Acid (^{13}C, ^{15}N) (Q)	Glu (^{13}C, ^{15}N)	148.1/104.3	-50	-18	-9
Glutamic Acid (^{13}C, ^{15}N) (C)	Glu (^{13}C, ^{15}N)	148.1/130.2	-50	-16	-5

Matrixmatched calibration standards prepared in synthetic urine further failed to adequately compensate for ion suppression in the FusionRP column. While enhanced polar selectivity and reduced total method time were desirable, the FusionRP column was ultimately not used in the method due to poor spike recoveries in real samples, likely resulting from the retention of undetected matrix components. In contrast, the run-to-run time for this method using a comparable HydroRP column was about 2 min longer, owing to the increased hydrophobic and steric interactions in the HydroRP phase. While preliminary studies favored the FusionRP column due to its efficiency, the spike recoveries obtained using the polar HydroRP column were far superior (81−124%). This indicates that the HydroRP column successfully separated the matrix components of the urine from the target analytes, making it the superior choice for optimal separation and sensitivity of this method. Acetonitrile was selected as the organic phase in the chromatographic separations due to the minimal background noise observed in the monitored mass transitions when compared with methanol. A mobile phase gradient was developed to optimize peak shape and separation. Figure 2 shows a representative chromatogram of the analytical standards prepared in synthetic urine and Figure 3 shows a representative chromatogram of the urine sample from a healthy individual volunteer. The optimized HPLC method was characterized by a low background signal and acceptable peak separation. The exceptions were MetSO/Glu and NAA/ pyruvic acid, which were partially separated from each other chromatographically. However, these compounds were detected with the mass spectrometer at different transitions.

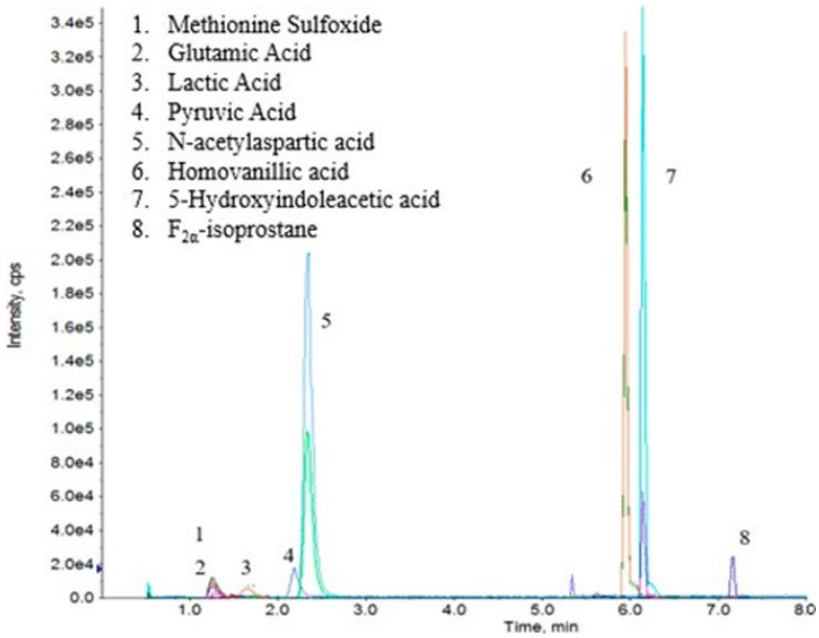

Figure 2. Representative overlaid XIC chromatogram of the eight metabolite standards prepared at 500 ug/L in synthetic urine.

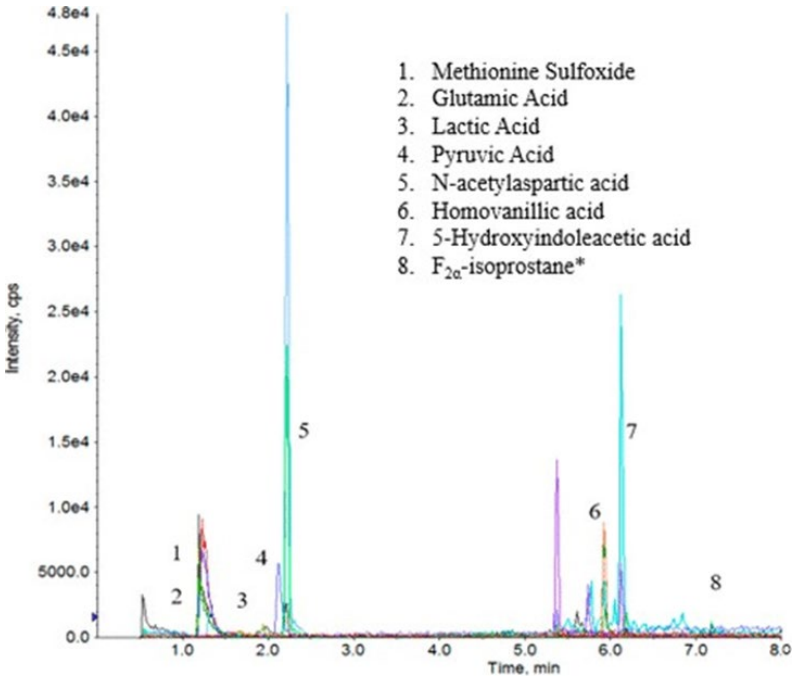

Figure 3. Representative overlaid XIC chromatogram of the eight metabolite standards in a urine specimen.

3.3. METHOD PERFORMANCE/VALIDATION

The performance characteristics of the newly optimized method were then determined, which have been summarized in Table 2. The method was found to have excellent sensitivity with method detection limits (MDLs) and limits of quantification (LOQ) comparable or superior to previously reported analytical methods that determined selected analytes studied here.34−39 The signal response further exhibited excellent linearity (R2 > 0.99) over a linear range applicable to biological specimens. All compounds were linear up to 500 μg/L, and most were linear up to 1000 μg/L. Method accuracy and reproducibility were significantly improved through the use of matrix-matched calibration standards as well as a stable isotope labeled internal standard of glutamic acid (13C, 15N) for glutamic acid detection only to improve its spike recovery. As a result, spike recoveries for all analytes in 200-fold diluted urine were between 80% and 120% (Table 3). Replicate measurements of recovery values yielded RSD values mostly <10% except Glu with a RSD 12.2%, which further indicates that the method performance was consistent and repeatable across urine samples. The authors note that use of additional internal standards would have yielded a more robust method. While having more isotope-labeled internal standards would be ideal, the satisfactory spike recoveries for these analytes reduced the need for additional and costly internal standards, and isotope labeled internal standards for several analytes were not commercially available. The performance characteristics shown here suggest that the newly developed method is sensitive, accurate, and rapid.

Table 2. HPLC-MS/MS Performance Characteristics

Analyte	Linear Range (μg/L)	R^2	LOD (μg/L)*	RT (min)
MetSO	5-1000	0.9936	5	1.23
Glu	5-1000	0.9999	5	1.27
Lac	20-1000	0.9952	20	1.64
Pyr	20-1000	0.9997	20	2.01
NAA	1-500	0.9998	1	2.07
HVA	1-1000	0.9992	1	5.99
5-HIAA	1-500	0.9982	1	6.21
$F_{2\alpha}$	1-500	0.9992	1	7.22

*LOD: Limits of detection were defined here as a signal-to-noise ratio (SNR) of 10.

3.4. APPLICATION TO URINE SPECIMENS

The newly developed HPLC-MS/MS method was ultimately applied to 12 urine specimens obtained from healthy university student volunteers. Each of the target compounds, with the exception of F2αisoprostane, was successfully detected and quantified in 11 of 12 urine specimens. F2α-isoprostane has been previously reported to occur at trace levels near 1 μg/L in urine,39 which fell below the limit of quantitation for this method.

Table 3. Results of spike recoveries and relative standard deviation (%RSD) values by spiking two different concentrations of potential TBI biomarkers in urine samples (n=4).

	Spike concentration 20 mg/L		Spike concentration 40 mg/L	
Analyte	Recovery	RSD	Recovery	RSD
MetSO	96.31	9.3	104.22	11.1
Glu	95.42	12.2	104.23	10.8
Lac	95.54	8.4	96.59	8.3
Pyr	89.45	8.8	91.57	8.6
NAA	81.37	4.8	86.14	4.1
HVA	89.15	6.6	107.77	5.4
5-HIAA	104.01	3.8	106.10	3.7
F_{2a}	111.80	6.3	124.52	5.7

Attempts to lessen the dilution factor to enable F2α-isoprostane quantitation resulted in increased ion suppression and decreased spike recoveries for most compounds, with the exception of pyruvate, which could be reliably measured at 50- fold dilution without significant performance loss. Nevertheless, the concentration ranges measured in this study generally agreed with the urinary ranges reported in the literature (Table 4).34−39

Table 4. Urinary concentrations of the potential TBI biomarkers in the 12 urine samples.

Analyte	Concentration Range (mg/L)	Mean concentration (mg/L)	Literature reported range (mg/L)[33-39]
MetSO	0.63-4.26	0.98	0.18-1.36
Glu	2.48-27.25	10.33	2.60-19.50
Lac	0.11-18.29	6.26	12.76-95.56
Pyr	2.36-5.84*	3.02	6.23-46.69
NAA	0.61-8.01	4.06	1.86-13.93
HVA	0.10-7.13	2.47	1.93-14.93
5-HIAA	0.31-1.95	0.64	2.03-15.21
$F_{2\alpha}$-Isoprostane	<LOD	<LOD	0.25-1.88

*Pyruvate concentrations were determined by 50-fold dilution

4. CONCLUSIONS

In this study, a simple, high-throughput HPLC-MS/MS method was developed to simultaneously determine eight urinary metabolites previously associated with TBI. This method is unique in its ability to simultaneously monitor these putative TBI biomarkers in a single analysis and without extensive sample preparation and preconcentration. The new method was rigorously optimized and validated to ensure its applicability to the analysis of clinical urine specimens, with method sensitivity and reproducibility comparable or superior to existing methods that may include selected metabolites studied here. The final application to clinical urine specimens found urinary concentrations that were in general agreement with previously reported concentrations for these metabolites.

In summary, this newly described method can accurately and rapidly quantify eight urinary metabolites simultaneously in the support of future clinical research to objectively characterize TBI using molecular biomarkers.

5. AUTHOR INFORMATION

5.1. CORRESPONDING AUTHORS

Casey Burton - Department of Chemistry, Missouri University of Science and Technology, Rolla, Missouri 65409, United States; Phelps Health, Rolla, Missouri 65401, United States; Orcidhttp://orcid.org/0000-0002-0729-6743; Email: c.f.burton@mst.edu

Honglan Shi - Department of Chemistry, Missouri University of Science and Technology, Rolla, Missouri 65409, United States; Orcidhttp://orcid.org/0000-0002-0801-5683; Email: honglan@mst.edu

5.2. AUTHORS

Austin Sigler - Department of Chemistry, Missouri University of Science and Technology, Rolla, Missouri 65409, United States

Xiaolong He - Department of Chemistry, Missouri University of Science and Technology, Rolla, Missouri 65409, United States

Mousumi Bose - Department of Chemistry, Missouri University of Science and Technology, Rolla, Missouri 65409, United States

Alexandre Cristea - Department of Chemistry, Missouri University of Science and Technology, Rolla, Missouri 65409, United States

Wenyan Liu - Department of Chemistry, Missouri University of Science and Technology, Rolla, Missouri 65409, United States

Paul Ki-souk Nam - Department of Chemistry, Missouri University of Science and Technology, Rolla, Missouri 65409, United States; Orcidhttp://orcid.org/0000-0002-6064-3257

Donald James - Phelps Health, Rolla, Missouri 65401, United States

5.3. NOTES

The authors declare no competing financial interest.

ACKNOWLEDGEMENTS

This study was sponsored by the Leonard Wood Institute in cooperation with the U.S. Army Research Laboratory and was accomplished under Cooperative Agreement Number W911NF-14-2-0034. The views and conclusions contained in this document are those of the authors and should not be interpreted as representing the official policies, either expressed or implied, of the Leonard Wood Institute, the Army Research Laboratory or the U.S. Government. The U.S. Government is authorized to reproduce and distribute reprints for Government purposes notwithstanding any copyright notation herein.

REFERENCES

1. Voss, J. D.; Connolly, J.; Schwab, K. A.; Scher, A. I. Update on the epidemiology of concussion/mild traumatic brain injury. Current pain and headache reports 2015, 19, 1-8.

2. McCrea, M.; Pliskin, N.; Barth, J.; Cox, D.; Fink, J.; French, L.; Hammeke, T.; Hess, D.; Hopewell, A.; Orme, D.; Powell, M.; Ruff, R.; Schrock, B.; Terryberry-Spohr, L.; Vanderploeg, R.; Yoash-Gantz, R.; Official Position of the Military TBI Task Force on the Role of Neuropsychology and Rehabilitation Psychology in the Evaluation, Management, and Research of Military Veterans with Traumatic Brain Injury. Clin Neuropsychol 2011, 22, 10-26.

3. Shenton, M.; Hamoda, H.; Schneiderman, J.; Bouix, S.; Pasternak, O.; Rathi, Y.; Vu, M.-A.; Purohit, M.; Helmer, K.; Koerte, I. A review of magnetic resonance imaging and diffusion tensor imaging findings in mild traumatic brain injury. Brain imaging and behavior 2012, 6, 137-192.

4. McCrory, P.; Meeuwisse, W. H.; Aubry, M.; Cantu, B.; Dvořák, J.; Echemendia, R. J.; Engebretsen, L.; Johnston, K.; Kutcher, J. S.; Raftery, M. Consensus statement on concussion in sport: the 4th International Conference on Concussion in Sport held in Zurich, November 2012. Br. J. Sports Med. 2013, 47, 250-258.

5. Singh, B.; Murad, M. H.; Prokop, L. J.; Erwin, P. J.; Wang, Z.; Mommer, S. K.; Mascarenhas, S. S.; Parsaik, A. K. Meta-analysis of Glasgow coma scale and simplified motor score in predicting traumatic brain injury outcomes. Brain Inj. 2013, 27, 293-300.

6. Shenton, M. E., Hamoda, H. M., Scheiderman, J. S., Bouix, S., Pasternak, O., Rathi, Y., Vu, M. A., Purohit, M. P., Helmer, K., Koerte, I., Lin, A. P., Westin, C. F., Kikinis, R., Kubicki, M., Stern, R. A., Zafonte, R., A review of magnetic resonance imaging and diffusion tensor imaging findings in mild traumatic brain injury. Brain Imaging Behav. 2012, 6, 137-192, DOI: 10.1007/s11682-012-9156-5.

7. Yuh, E. L.; Mukherjee, P.; Lingsma, H. F.; Yue, J. K.; Ferguson, A. R.; Gordon, W. A.; Valadka, A. B.; Schnyer, D. M.; Okonkwo, D. O.; Maas, A. I. Magnetic resonance imaging improves 3- month outcome prediction in mild traumatic brain injury. Annals of neurology 2013, 73, 224-235.

8. Asken B. M.; DeKosky, S. T.; Clugston, J. R.; Jaffee, M. S.; Bauer, R. M.; Diffusion tensor imaging (DTI) findings in adult civilian, military, and sport-related mild traumatic brain injury (mTBI): a systematic critical review. Brain Imaging Behav 2019, 12, 585-612, DOI: 10.1007/S11682-017-9708-9

9. Luan, H., Liu, L., Meng, N., Tang, Z., Chua, K., Chen, L., Song, J., Mok, V.C.T., Xie, L., Li, M., Cai, Z., LC-MS-Based Urinary Metabolite Signatures in Idiopathic Parkinson's Disease, J. Proteome Res. 2015 14, 1, 467-478, DOI: 10.1021/PR500807T

10. Vos, P.; Jacobs, B.; Andriessen, T.; Lamers, K.; Borm, G.; Beems, T.; Edwards, M.; Rosmalen, C.; Vissers, J. GFAP and S100B are biomarkers of traumatic brain injury An observational cohort study. Neurology 2010, 75, 1786-1793.

11. Honda, M.; Tsuruta, R.; Kaneko, T.; Kasaoka, S.; Yagi, T.; Todani, M.; Fujita, M.; Izumi, T.; Maekawa, T. Serum glial fibrillary acidic protein is a highly specific biomarker for traumatic brain injury in humans compared with S-100B and neuron-specific enolase. Journal of Trauma and Acute Care Surgery 2010, 69, 104-109.

12. De Kruijk, J.; Leffers, P.; Menheere, P.; Meerhoff, S.; Twijnstra, A. S- 100B and neuron specific enolase in serum of mild traumatic brain injury patients A comparison with healthy controls. Acta neurologica scandinavica 2001, 103, 175-179.

13. Honda, M.; Tsuruta, R.; Kaneko, T.; Kasaoka, S.; Yagi, T.; Todani, M.; Fujita, M.; Izumi, T.; Maekawa, T.; Serum glial fibrillary acidic protein is a highly specific biomarker for traumatic brain injury in humans compared with S-100B and neuron-specific enolase. J. Trauma, 2010, 69, 104-109.

14. Bulut, M.; Koksal, O.; Dogan, S.; Bolca, N.; Ozguc, H.; Korfali, E.; Ilcol, Y.; Parlak, M. Tau protein as a serum marker of brain damage in mild traumatic brain injury: preliminary results. Advances in therapy 2006, 23, 12-22.

15. Papa, L.; Akinyi, L.; Liu, M. C.; Pineda, J. A.; Tepas III, J. J.; Oli, M. W.; Zheng, W.; Robinson, G.; Robicsek, S. A.; Gabrielli, A. Ubiquitin C-terminal hydrolase is a novel biomarker in humans for severe traumatic brain injury. Critical care medicine 2010, 38, 138.

16. Papa, L.; Lewis, L. M.; Silvestri, S.; Falk, J. L.; Giordano, P.; Brophy, G. M.; Demery, J. A.; Liu, M. C.; Mo, J.; Akinyi, L. Serum levels of ubiquitin C-terminal hydrolase distinguish mild traumatic brain injury from trauma controls and are elevated in mild and moderate traumatic brain injury patients with intracranial lesions and neurosurgical intervention. Journal of Trauma and Acute Care Surgery, 2012, 72, 1335-1344.

17. MacFarlane, M. P.; Glenn, T. C. Neurochemical cascade of concussion. Brain injury 2015, 29, 139-153.

18. Barkhoudarian, G.; Hodva, D. A., Giza, C. G., The Molecular Pathophysiology of Concussive Brain Injury, Clin. Sports. Med., 2011, 30, 33-48.

19. Wagner, A. K.; Ren, D.; Conley, Y. P.; Ma, X.; Kerr, M. E.; Zafonte, R. D.; Puccio, A. M.; Marion, D. W.; Dixon, C. E. Sex and genetic associations with cerebrospinal fluid dopamine and metabolite production after severe traumatic brain injury. Journal of neurosurgery 2007, 106, 538-547.

20. Katayama, Y.; Becker, D. P.; Tamura, T.; Hovda, D. A. Massive increases in extracellular potassium and the indiscriminate release of glutamate following concussive brain injury. Journal of neurosurgery 1990, 73, 889-900.

21. Aquilani, R.; Iadarola, P.; Boschi, F.; Pistarini, C.; Arcidiaco, P.; Contardi, A. Reduced plasma levels of tyrosine, precursor of brain catecholamines, and of essential amino acids in patients with severe traumatic brain injury after rehabilitation. Archives of physical medicine and rehabilitation 2003, 84, 1258-1265.

22. Vespa, P. M.; McArthur, D.; O'Phelan, K.; Glenn, T.; Etchepare, M.; Kelly, D.; Bergsneider, M.; Martin, N. A.; Hovda, D. A. Persistently Low Extracellular Glucose Correlates With Poor Outcome 6 Months After Human Traumatic Brain Injury Despite a Lack of Increased Lactate & colon; A Microdialysis Study. Journal of Cerebral Blood Flow & Metabolism 2003, 23, 865-877.

23. Yang MS, Dewitt DS, Becker DP, Hayes RL. Regional brain metabolite levels following mild experimental head injury in the cat. Journal of Neurosurgery 1985, 63, 617.

24. Inao S, Marmarou A, Clarke GD, Andersen BJ, Fatouros PP, Young HF. Production and clearance of lactate from brain tissue cerebro-spinal fluid and serum following experimental brain injury. Journal of Neurosurgery 1988, 69, 736.

25. Narayanan, S.; De Stefano, N.; Francis, G. S.; Arnaoutelis, R.; Caramanos, Z.; Collins, D. L.; Pelletier, D.; Arnason, B. G.; Antel, J. P.; Arnold, D. L. Axonal metabolic recovery in multiple sclerosis patients treated with interferon β–1b. Journal of neurology 2001, 248, 979-986.

26. Yeo, R. A.; Phillips, J. P.; Jung, R. E.; Brown, A. J.; Campbell, R. C.; Brooks, W. M. Magnetic resonance spectroscopy detects brain injury and predicts cognitive functioning in children with brain injuries. Journal of neurotrauma 2006, 23, 1427-1435.

27. Sharma, R.; Laskowitz, D. T. Biomarkers in traumatic brain injury. Current neurology and neuroscience reports 2012, 12, 560-569.

28. Varma, S.; Janesko, K. L.; Wisniewski, S. R.; Bayir, H.; Adelson, P. D.; Thomas, N. J.; Kochanek, P. M. F2-isoprostane and neuron-specific enolase in cerebrospinal fluid after severe traumatic brain injury in infants and children. Journal of neurotrauma 2003, 20, 781-786.

29. Zetterberg, H., Smith, D. H., Blennow, K., Biomarkers of mild traumatic brain injury in cerebrospinal fluid and blood. Nature Reviews Neurology 2013, 9, 201–210

30. Bouatra S, Aziat F, Mandal R, Guo AC, Wilson MR, Knox C, Bjorndahl, T. C., Krishnamurthy, R., Saleem, F., Liu, P., Dame, Z. T., Poelzer, J., Huynh, J., Yallou, F. S., Psychogios, N., Dong, E., Bogumil, R., Roehring, C., Wishart, D. S., The Human Urine Metabolome. PloS one 2013, 8, 9, DOI: 10.1371/journal.pone.0073076

31. Kvitvang H. F., Andreassen T, Adam T, Villas-Boas S. G., Bruheim P, Highly sensitive GC/MS/MS method for quantitation of amino and nonamino organic acids. Anal. Chem. 2011, 83, 2705-2711. DOI: 10.1021/ac103245b.

32. Jones MG, Cooper E, Amjad S, Goodwin CS, Barron JL, Chalmers RA: Urinary and plasma organic acids and amino acids in chronic fatigue syndrome. Clin. Chim. Acta. 2005, 61, 150-158. DOI: 10.1016/j.cccn.2005.05.023

33. A. E. Stroomer, H. Overmars, N. G. Abeling, A. H. van Gennip, Simultaneous determination of acidic 3,4-dihydroxyphenylalanine metabolites and 5-hydroxyindole-3- acetic acid in urine by high-performance liquid chromatography. Clin. Chem. 1990, 36, 1834-1837.

34. Achaintre D., Bulete A., Cren-Olive C., Li L., Rinaldi S., Scalbert A., Differential Isotope Labeling of 38 Dietary Polyphenols and Their Quantification in Urine by Liquid Chromatography Electrospray Ionization Tandem Mass Spectrometry. Anal. Chem. 2016, 88, 2637-2644. DOI: 10.1021/acs.analchem.5b03609.

35. Guo K, Li L, Differential 12C-/13C-isotope dansylation labeling and fast liquid chromatography/mass spectrometry for absolute and relative quantification of the metabolome. Anal. Chem. 2009, 81, 3919-3932. DOI: 10.1021/ac900166a.

36. Basu S, Radioimmunoassay of 8-iso-prostaglandin F2alpha: an index for oxidative injury via free radical catalysed lipid peroxidation. Prostaglandins Leukot Essent Fatty Acids. 1998, 58, 319-325. DOI: 10.1016/s0952-3278(98)90042-4

37. Burton, C., Shi, H., Ma, Y. Normalization of urinary pteridines by urine specific gravity for early cancer detection. Clin. Chim. Acta, 2014, 435, 42-47.

38. Wu, Z.; Gao, W.; Phelps, M. A.; Wu, D.; Miller, D. D., Dalton, J. T.; Favorable Effects of Weak Acids on Negative-Ion Electrospray Ionization Mass Spectrometry, Anal. Chem., 2004, 76, 839-847.

39. Sánchez-Rabaneda, F.; Jáuregui, O.; Casals, I.; Andrés-Lacueva, C., Izquierdo-Pulido, M.; Lamuela-Raventós, R. M.; Liquid chromatographic/electrospray ionization tandem mass spectrometric study of the phenolic composition of cocoa (Theobroma cacao), J. Mass Spectrom., 2003, 38, 35-42.

II. REPEATED LOW LEVEL BLAST EXPOSURE ALTERS URINARY AND SERUM METABOLITES

Austin Sigler1, Jiandong Wu1, Annalise Pfaff,1 Olajide Adetunji,1 Paul Ki-souk Nam1, Donald James2, Casey Burton1, 2*, Honglan Shi1*

Deparment of Chemistry, Missouri University of Science and Technology, Rolla, MO 65409

Correspondance:

Casey Burton - Department of Chemistry, Missouri University of Science and Technology, Rolla, Missouri 65409, United States; Phelps Health, Rolla, Missouri 65401, United States; Orcid: http://orcid.org/0000-0002-0729-6743; Email: c.f.burton@mst.edu

Honglan Shi - Department of Chemistry, Missouri University of Science and Technology, Rolla, Missouri 65409, United States; Orcid: http://orcid.org/0000-0002-0801-5683; Email: honglan@mst.edu

ABSTRACT

Repeated exposure to low-level blast overpressures can produce biological changes and clinical sequelae that resemble mild traumatic brain injury (TBI). While recent efforts have revealed sev-eral protein biomarkers for axonal injury during repetitive blast exposure, this study aims to ex-plore potential small molecule biomarkers of brain injury during repeated blast exposure. This study evaluated a panel of ten small molecule metabolites involved in neurotransmission, oxida-tive stress, and energy metabolism in the urine and serum of military personnel (n = 27) con-ducting breacher training with repeated exposure to low-level blasts. The metabolites were ana-lyzed using HPLC – tandem mass spectrometry and Wilcoxon signed rank test was used for sta-tistical analysis to compare between the levels of pre-blast and post-blast exposures.

Urinary levels of homovanillic acid ($P < 0.0001$), linoleic acid ($P = 0.0030$), glutamate ($P= 0.0027$), and serum N-acetylaspartic acid ($P = 0.0006$) were found to be significantly altered following repeated blast exposure. Homovanillic acid concentration was also found continue to decrease with increased repeat exposure. These results suggest that repeated low-level blast exposures can produce measurable changes in urine and serum metabolites that may aid in identifying individuals at increased risk of sustaining a TBI. Larger clinical studies are needed to extend the generalizability of these findings.

Keywords: blast exposure, TBI, metabolites, homovanillic acid

1. INTRODUCTION

Military personnel encounter repeated low-level blast exposures in the course of training and combat operations [1, 2]. Repeated low-level blast exposures can produce biological and clinical changes that resemble mild traumatic brain injury (TBI), which has prompted interest in the long-term effects of blast exposure on neurodegeneration [3]. For example, the cumulative effect of repeated blast exposure can be evidenced by clinical symptomology [4], neuroimaging [5, 6], and an increased incidence of post-traumatic stress disorder, various dementias, and long-term neurological deficits [7, 8]. In the short term, brain injuries resulting from repeated low-level blast exposures or other repetitive mild brain injury can further increase the risk of repeat injury upon subsequent exposures [5, 9]. As a result, suspected brain injuries caused by blast ex-posures need to be assessed for medical intervention in a timely manner to mitigate long-term health consequences. In current clinical practice, suspected blast-induced brain injuries are

evaluated using an array of neuropsychological evaluations, acute injury surveillance, and imaging studies [10]. The primary drawbacks of these approaches include subjectivity, insensi- tivity to mild injuries, and poor applicability in the field, leading to delayed diagnosis, inadequate treatment, and increased risk of developing long-term neurological deficits. In response, recent studies have begun to explore the underlying biological and chem-ical changes in pursuit of novel molecular biomarkers that can be used to better assess and characterize blast-induced brain injury [11, 12]. Altered levels of several proteins, such as neuron-specific enolase, S100B, and glial fibrillary acidic protein, have been reported in serum and cerebrospinal fluid (CSF) [13-16]. While CSF poses practical challenges for routine screening, owing to its poor accessibility, serum proteins offer a new tool for assessing brain trauma. Similarly, recent efforts have found suggestive evidence that certain serum proteins may become altered following repetitive blast exposures [17].

However, the limited number of serum proteins that have been identi-fied to date combined with their limited specificity to brain injury has encouraged the pursuit of additional molecular biomarkers to provide detailed characterization of the nature of a given brain injury. This provides impetus to explore how low-level repeat blast exposures may produce measurable changes of small molecular biomarkers.

Urinary metabolites present a novel direction for blast-related biomarker devel-opment. Urine as a biofluid offers ease of accessibility, ample sample volume, and a relatively simple matrix. The research of urinary biomarkers for brain diseases are in-creasing as reviewed by An and Gao [18], but only very limited studies have explored urinary biomarkers for brain injury. The addition of urinary metabolites to the suite of

tools currently available could provide clinicians with pertinent information about the distinct pathology of a given brain injury. To this end, we have recently developed a highly sensitive high-performance liquid chromatography-tandem mass spectrometry (HPLC-MS/MS) method to detect a panel of urinary metabolites related to several distinct pathological processes involved in brain injury [19]. The panel included homovanillic acid (HVA), glutamic acid/glutamate (Glu), lactic acid (Lac), linoleic acid (LA), Arachidonic acid (AA), pyruvic acid (Pyr), methionine sulfoxide (MetSO), N-acetylaspartic acid (NAA), 5-hydroxyindoleacetic acid (5-HIAA), and F2α-isoprostane (F2α). Specifically, Glu is the primary excitatory neurotransmitter in the brain, and the excessive glutamatergic release that follows a concussive blow pre-cipitates a cascade of detrimental effects that can lead to long-term neurological effects [20]. Similarly, altered levels of other neurotransmitters and their metabolites in cere-brospinal fluid, such as HVA and 5-HIAA, can indicate dysregulated neurotransmission following a brain injury [20]. NAA is highly abundant in brain tissue and disruptions to the blood brain barrier and breakdown of brain tissue may lead to its subsequent in-crease in serum. Elevated levels of MetSO, the oxidized form of the essential amino acid methionine, in serum have been associated with oxidative stress [21]. Metabolic dysregulation can additionally accompany TBI causing altered levels of Lac and Pyrd [22]. Finally, fatty acids, such as LA and AA, are enriched in neuronal and oligoden-drocytic membranes. Changes in fatty acid levels can be indicative of neuronal cell damage, disruption of the blood brain barrier, oxidative stress, and inflammation [23]. Together, this panel of metabolites can monitor and detect changes in several distinct biological and pathological mechanisms associated with blast-related TBI. In the current study, a novel panel of metabolites was

evaluated in a longitudinal study to assess their changes in both urine and serum following repeated low-level blast exposure. The study was performed at The Urban Mobility Breacher Course at Fort Leonard Wood, Missouri, USA, which is a training program in which military personnel are trained to breach buildings using explosive devices. Trainees are subjected to dozens of blasts involving light charges (0.03, 0.07, 0.11, and 0.15 lbs C4) and heavy charges (10.44 lbs C4) over the course of several days. Low intensity blast exposure has already been implicated in both behavioral and structural brain abnormalities in mice [24], and this training provides a unique opportunity to assess changes through a metabolic panel in humans. This novel experimental design was selected to provide unique insights into how repeated low-level blast exposure alters metabolism and whether specific metab-olites, alone or in combination, may have clinical value in the risk assessment and characterization of blast-related brain injury.

2. MATERIALS AND METHODS

2.1. MATERIALS

All chemicals and solvents were high purity (<97% or better). Chemical standards for HVA, Glu, Lac, Pyr, MetSO, NAA, AA, LA, isotopically-labeled internal standards glutamic acid-13C5,15N (Glu-13C5,15N), 5-hydroxyindoleacetic acid 4,6,7 D3-acetic-3-D2 (5-HIAA-D5), and N-acetyl-L-aspartic acid-2,3,3-D3 (NAA-D3) were purchased from Sigma-Aldrich, (St. Louis, MO, USA). In addition, 5-HIAA, F2α, LC-MS-grade methanol, isopropanol, acetonitrile (ACN), and optima™ grade formic acid (FA) were

purchased from Fischer Scientific (Hampton, NH, USA). Isotopically labeled internal standard F2α-isoprostane-D4 (F2α- D4) was purchased from Cayman Chemicals (Ann Arbor, Michigan, USA). Ultrapure water (18.2 MΩ.cm) was generated in-house by a Millipore Elix-3 purification system (Millipore, Billerica, MA, USA).

2.2. PARTICIPANTS AND SPECIMENS

A total of 27 active military personnel (25 males and two females, age range: 20-35) were recruited to participate in this study from the Urban Mobility Breacher Course at Fort Leonard Wood, MO, USA in June 2021. The research protocol and informed consent process for the study were approved by the Phelps Health Institutional Review Board (IRB), University of Missouri IRB, and the Human Research Protection Program of the Army Research Laboratory. The Urban Mobility Breacher Course consisted of a two-week training course with the first week comprising classroom-based learning and the second week comprising field exercises involving repeat blast exposures. Figure 1 shows blast exposures and sample collections. Prior to blasting, three daily spot urine specimens consisting of first or second morning voids were collected from each par-ticipant. Additionally, a 5 mL blood specimen was obtained on the first day of sample collection prior to blasting. Three additional daily spot urine specimens consisting of first or second morning voids were collected after blast exposures of each day. Finally, a 5 mL blood specimen was collected on the final day of sample collection. Blast speci-mens were collected approximately 16 hours after the previous day's blast exposures. The blood specimens were spun down after 30 min clotting time and serums were col-lected, aliquoted, and frozen immediately at –80 oC until analysis. The urine samples were

frozen immediately in a deep freezer at -80 °C on the collection site and transferred to Missouri University of Science and Technology for analysis. Urine specimens were subsequently thawed, aliquoted, and refrozen at -80 °C until analysis, except for one urine aliquot per specimen to determine urine specific gravity.

Figure 1 Urban Mobility Breacher Course blast exposure and sample collection scuedules.

2.3. SAMPLE PREPARATION

The sample preparation was performed by following our published method [19] with slight modification to include more internal standards to further improve robustness of the method for HPLC-MS/MS method 1 analysis. Briefly, after specimens were thawed and equilibrated to room temperature, each 100 µL aliquot was added to 900 µL mixture of 800 µL ACN and 100 µL ultrapure water containing 10 mg/L of internal standards 5-HIAA-D5, Glu-13C5,15N, NAA-D3, and F2α-D4 in a 1.5 mL microcentrifuge tubes and processed and analyzed by HPLC-MS/MS by following the published procedure [19].

2.4. HPLC-MS/MS METHODS

Each sample was analyzed using two previously described HPLC-MS/MS methods to quantify the ten metabolites in this study [19, 25]. -The same UFLC coupled to a 4000 Q-TRAP tandem mass spectrometer (AB SCIEX, Concord, ON, CA) was used for both HPLC-MS/MS methods. The first HPLC-MS/MS method analyzed the eight metabolites was same as our previously published method [19] with further improvement of method robustness by including additional isotope labelled internal standards. The second method for quantifying LA and AA was adapted from a published method [25]. The method was slightly modified to reduce the HPLC-MS/MS analysis time. Briefly, an Ascentis Express C18 column (10 cm × 2.1 mm, 2.7 μm particle size, Phenomenex) was used. The analytes were eluted with a flow rate set to 0.3 mL/min under a gradient elution program with eluent A (3:2 ultrapure water:ACN with 10 mM ammonium ace- tate and 0.1% formic acid) and eluent B (9:1 isopropanol:ACN with 10 mM ammonium acetate and 0.1% FA) . The gradient began with 20% B, followed by a linear increase over 3 minutes to 100% B which was maintained for 2.5 minutes before decreasing to 20% B over 0.5 minutes and equilibrated at 20% B for 10 minutes before next injection. Opti- mized ion source conditions were: ion source temperature of 400 °C, ion spray voltage of -4500 V, curtain gas pressure at 15 psi, ion source gas 1 pressure at 50 psi, and ion source gas 2 pressure at 30 psi. The mass transitions and optimized other conditions are listed in Table 1.

Table 1. Optimized parameters for Method 2. The upper ion pairs were used for quantification while the lower ion pairs were used for confirmation.

Compound	Ion Pairs	Declustering Potential (DP, V)	Collision Energy (CE, V)	Collision Cell Exit Potential (CXP, V)
Arachidonic Acid (AA)	349.4/303.6 349.4/259.6	-35 -35	-18 -24	-7 -17
Linoleic Acid (LA)	325.4/279.6 325.4/45.2	-30 -30	-18 -30	-7 -1

Both HPLC-MS/MS methods were validated to make sure certified performance in urine and serum samples before applying for analyses of field blast samples.

2.5. URINE SPECIFIC GRAVITY MEASUREMENTS

Urinary metabolite concentrations were normalized to urine concentration-dilution to account for an individual's hydration status and time since last urination using urine specific gravity (USG). USG was measured refractometrically with a Reichert digital Clinic-Chek Digital Handheld Refractometer after urine specimens equilibrated to room temperature [26].

2.6. QUALITY ASSURANCE AND QUALITY CONTROL

All analytical methods were validated prior to sample analysis. These include analyses of blanks, calibration standards, method detection limits, reproducibility of replicate samples, and sample matrix spikes. During sample analysis, one or more blank, dupli-cate of samples, and sample spike recovery checks were performed for each batch

of samples to make sure that all data were of good quality. Samples initially with concentration above the calibration range were diluted and reanalyzed.

2.7. DATA HANDLING AND STATISTICAL ANALYSIS

USG-adjusted analyte concentrations were expressed in μg/L. Analyte concentrations below the limit of quantification (LOQ) were treated as zero for statistical analysis. Statistical analyses were conducted using GraphPad Prism 9 (San Diego, CA). Non-parametric Wilcoxon signed rank tests were performed using untransformed analyte levels from paired groups (urine or serum samples from the same participants pre- and post-blast exposure). Significance levels for Wilcoxon matched-pairs signed-rank tests were set at 0.05 (two-tailed).

3. RESULTS

3.1. ANALYTICAL METHODS PERFORMANCE

Both HPLC-MS/MS methods performed well in urine and serum samples with good accuracies and precisions. For Method 1, the relative standard deviations (RSD) for the eight urinary metabolites ranged from 2.7% to 6.7% and spiked recoveries ranged from 81.4% to 111.8%. The RSDs for the eight serum metabolites ranged from 2.4% to 9.4% and spiked recoveries ranged from 86.1% to 121.4%. For analysis of AA and LA (Method 2), the RSDs ranged from 1.6 to 4.2% in urine and from 3.4 to 4.2% in serum. The spiked recoveries ranged from 94.1% to 106% for urine and 103% to 108.7% for serum. The method quantification detection limit for LA was 10 μg/L in both urine and

serum. The method quantification detection limits for AA were 1 µg/L and 10 µg/L in urine and serum, respectively.

3.2. COMPARISON OF URINARY METABOLITES FOLLOWING BLAST EXPOSURE

Statistical comparisons using the average pre-blast and post-blast metabolite concen-trations for each participant were performed to examine the effects of blast exposures on urinary metabolite levels. Wilcoxon signed-rank comparisons revealed that significant changes occurred in urinary levels of LA, HVA, and Glu following blast exposure (Figure 2).

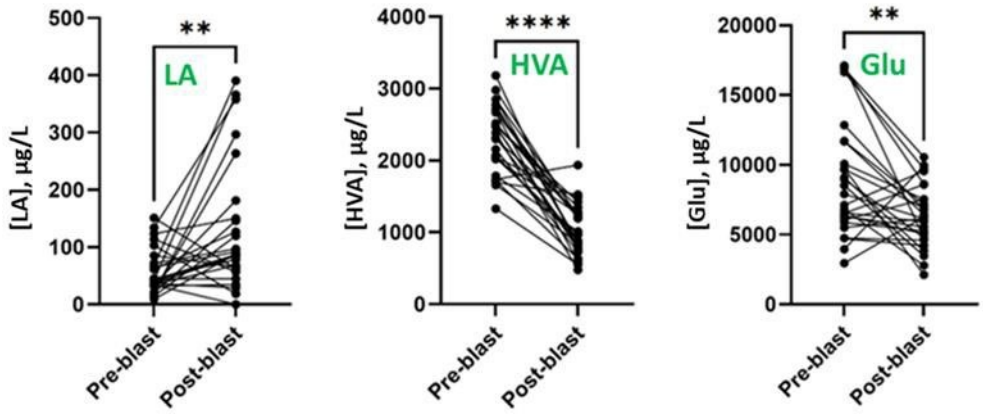

Figure 2. Pre- and post-blast LA, HVA, and Glu levels in urine for each participant (N=27). Black circles represent 3-day average, and lines connect pre- and post-blast levels for each participant. ** $p < 0.01$, **** $p < 0.0001$ determined by Wilcoxon matched pairs signed rank test.

The post-blast concentrations of HVA were significantly lower than the pre-blast levels (pre-blast median of 2385 µg/L versus post-blast median of 969.4 µg/L, $p<0.0001$). As the primary metabolite of dopamine, reduced levels of urinary HVA following blast

expo-sure may indicate altered neurotransmission [20] and dopamine formation in damaged neurons [27]. Dopamine systems including HVA have been widely implicated in cog-nitive deficits following TBI. For example, reduced dopamine transmission has been previously reported in plasma samples collected from rodent models using controlled cortical impact and fluid percussion techniques to induce traumatic brain injuries [28]. Decreased HVA has also been reported in human cerebrospinal fluid (CSF) after head injury [29, 30]. Interestingly, CSF levels of 5-HIAA were similarly found to be un-changed following head injuries despite decreased HVA [29, 30], same trend as we found in this study in urines of participants, 5-HIAA concentrations were not changed significantly pre- and post-blast exposures while HVA concentration decreased fol-lowing blast exposure. These results indicate that the urinary level alterations of HVA and 5-HIAA after blast exposure are similar with those in CSF from brain injury, sug-gesting that the repeat low-level blast exposure induces similar metabolic alterations with those from TBI. The similar repeated blast-related training also elevated protein biomarkers in serum of the participants, indicating axonal injury [17]. Further larger scale study to evaluate urinary HVA and serum proteins as potential TBI biomarkers may provide highly useful clinical diagnostic technique. Our temporal urinary experiment results showed that HVA level in urine continues to decrease with repeated blast exposure (Figure 3). Another recent pilot study has found that urinary HVA decreases following TBI up to six months and lower levels of HVA negatively correlated to injury severity [31]. Similarly, decline of HVA in CSF was more notable in patients with the longer duration of unconsciousness [29]. Together, it seems that HVA may not only be a potential brain injury biomarker, but it may also serve as a potential biomarker to

evaluate injury severity and recover status of the injury, in-cluding the mild TBI that is challenging to diagnose [32]. The key advantages of urinary HVA as biomarker are easy sample collection, ample volume of sample, simple matrix for analysis. It will be highly valuable and interesting for clinical application.

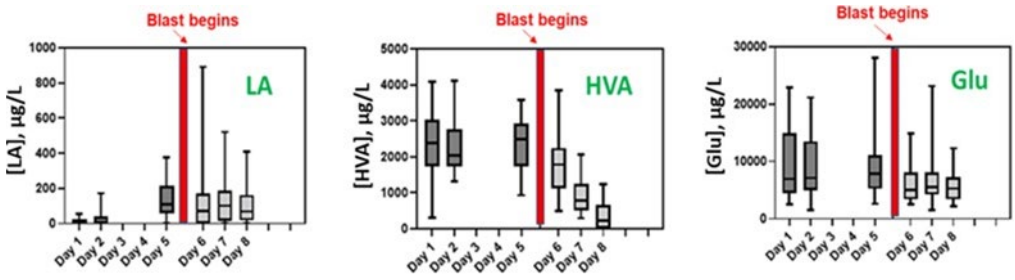

Figure 3. Box-and-whisker plots of LA, HVA, and Glu levels as a function of date collected. For each day urine was collected, the box represents the 25th-75th percentiles, with a horizonal bar at the median.

Urinary Glu levels also decreased significantly after blast exposures (pre-blast median of 7906 µg/L versus post-blast median of 6161 µg/L, $p = 0.0027$), though the change is not as drastic as HVA. The exposure time profile (Figure 3) did not show significant tem-poral change with increased blast exposure, suggesting the alteration of the Glu may not as sensitive as HVA under the subtle brain insults. It is also possible that altered Glu-glutamine metabolic conversion play a role during these blast exposures, but we did not measure glutamine concentration in our selected biomarker panel in this study. Nevertheless, decreased levels of urinary Glu, a primary neurotransmitter, further suggests altered neurotransmission following low-level repetitive blasts, and this al-teration is possibly diagnosed by urinary Glu as a biomarker. Previous microdialysis studies in both humans and rodents have shown an immediate rise in extracellular

glutamate levels following TBI while magnetic resonance spectroscopy (MRS) studies have shown a decrease in total glutamate in human brains following TBI [33].The im-balances of Glu are different for acute, subacute, and chronic changes following TBI [33]. Though the neuroscience research has provided insight into the mechanism of Glu following TBI, the biological alteration and mechanism are still not fully understood. Our current pilot study, as best of our knowledge, is the first to measure urinary Glu level in urine specimen of human subject during repeat blast exposure and repeat brain insults. It is highly desirable for larger scale studies to evaluate the possibility of Glu as a TBI biomarker by testing urine specimen.

In contrast, urinary LA levels significantly increased after blast exposure (pre-blast median of 42.7 μg/L, versus post-blast median of 173.9 μg/L, $p = 0.0030$). LA has been reported increased in brain following brain injury [34, 35, 36], indicating its involvement in response to the injury. However, little is known about the exact role of LA in brain. This post-blast increase of LA may similarly suggested altered neurotransmission through LA and/or LA metabolites that regulate brain signaling [34]. The same altera-tion trend of LA in urine and in brain suggested urinary LA change may serve as a much easier accessed biomarker of LA function and mechanism in brain injury. It should be noticed that large variations of LA concentrations among participants were observed. This might be due to the dietary differences of the participants as LA is the most con-sumed polyunsaturated fatty acid in the US diet [37]. The dietary consumptions of the participants were not recorded in this study and should be included or controlled in future investigation. In addition, the concentrations of LA are low and more variable because most of its excretion to urine are its metabolites. Although the

dietary con-sumption of the LA may affect its urinary level to challenge it as an individual bi-omarker, together with HVA and Glu in a panel, and with well controlled dietary intake, LA may still be a valuable compound in neuroscience research and related clinical applications. The pre- and post-blast exposure concentration median and ranges of all the urinary metabolites in our study panel have been summarized in Table 2. It should be noticed that urinary F2α was not meaningfully detected in this sample cohort and was excluded from data analysis. Pre-concentration methods may be used to better detect this analyte, although it was not employed in the current study owing to practical limitations.

Table 2. Pre- and post-blast levels (μg/L) of dilution-corrected urinary metabolites (N=27). P-values indicating a significant difference between pre- and post-blast samples are in bold.

Analyte	**Pre-blast Urine**		**Post-blast Urine**		**P-value**
	Median	Range	Median	Range	
Linoleic acid (LA)	42.7	<LOD–352	173.9	<LOD – 857	**0.0030**
Homovanillic acid (HVA)	2320	300–4108	864.6	<LOD–3850	**<0.0001**
Lactic acid (Lac)	933.7	65.18–2466	897.1	120.4–2724	0.7140
N-acetylaspartic acid (NAA)	5831	2784–9879	6638	3127–12926	0.2687
Arachidonic acid (AA)	18.82	6.045–59.14	26.87	8.483–81.41	0.2792
Pyruvic acid (Pyr)	1461	553.4–3731	1397	349.8–1959	0.2792
Methionine sulfoxide (MetSO)	105.2	11.91–398.6	138.6	61.54–302.3	0.1855
5-hydroxyindolea cetic acid (5-HIAA)	2776	1149–5515	2397	936.5–5157	0.9153
Glutamic acid (Glu)	7906	1927–27132	6161	2122–24891	**0.0027**

This was additionally limited by its sample size and restricted amount of blast exposure in this study design, which may have limited our ability to discern measurable changes in the other metabolites following blast exposure.

3.3. COMPARISON OF SERUM METABOLITES FOLLOWING BLAST EXPOSURE

Wilcoxon signed-rank analyses were similarly performed for serum concentrations of the metabolite panel. These comparisons revealed that serum NAA levels of pre-blast were significantly different from post-blast (pre-blast median of 107.3 μg/L versus a post-blast median of 136.5 μg/L, $p = 0.0006$) (Figure 4). As a highly abundant metabolite in brain tissue, decreased levels of NAA have been reported in the brain using MRS, suggesting potential leakage into the bloodstream [38]. The increased serum levels ob-served in the current study provides supporting evidence that NAA may leak into the bloodstream following brain injury. While serum levels have not previously been re-ported in the context of traumatic brain injury, increased serum levels of NAA have been reported in patients with amyotrophic laceral sclerosis characterized by the pro-gressive degeneration of nerve cells [39].

Regional reduction of NAA has also been used as a marker of neuronal or axonal loss in several neurological disorders and even TBI [40]. NAA derivatives have additionally been implicated in altered glutamatergic transmission [40]. The combined changes seen for urinary glutamate and serum NAA provides further evidence that repeated blast exposure may contribute to alterations in neurotransmission and the metabolites that normally regulate those processes.

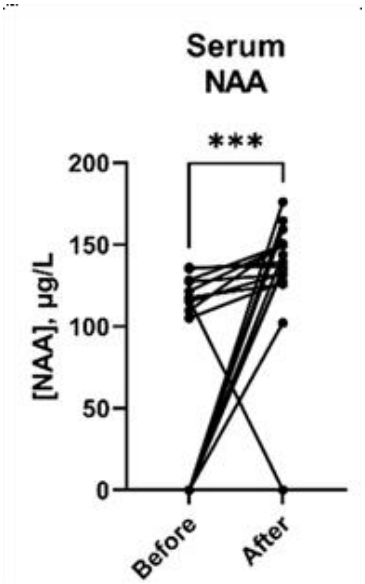

Figure 4. Pre- and post-blast NAA levels in serum for each participant (N=17). Black circles represent 3-day average, and lines connect pre- and post-blast levels for each participant. *** $p < 0.01$, determined by Wilcoxon matched pairs signed rank test.

The concentrations of all serum metabolites tested have been summarized in Table 3. Differences between urine and serum concentrations, including limited detection of certain metabolites in serum, may be attributed to different temporal profiles of metabolic changes following injury in different biofluids. In addition, urine samples were collected almost daily but serum samples were only collected at the beginning and end of the training represent only one time collection each pre- and post-blast exposure.

Furthermore, serum fatty acids were likely not appreciably detected in the current study as a result of the protein precipitation step during sample preparation. Serum fatty acids are found disproportionately bound to lipoproteins in the bloodstream, causing protein precipitation methods to inadvertently remove fatty acids from the sample [41].

Table 3. Pre- and post-blast levels (μg/L) of dilution-corrected urinary metabolites (N=27). P-values indicating a significant difference between pre- and post-blast samples are in bold.

Analyte	**Pre-blast Urine**		**Post-blast Urine**		**P-value**
	Median	Range	Median	Range	
Linoleic acid (LA)	42.7	<LOD–352	173.9	<LOD –857	**0.0030**
Homovanillic acid (HVA)	2320	300–4108	864.6	<LOD–3850	**<0.0001**
Lactic acid (Lac)	933.7	65.18–2466	897.1	120.4–2724	0.7140
N-acetylaspartic acid (NAA)	5831	2784–9879	6638	3127–12926	0.2687
Arachidonic acid (AA)	18.82	6.045–59.14	26.87	8.483–81.41	0.2792
Pyruvic acid (Pyr)	1461	553.4–3731	1397	349.8–1959	0.2792
Methionine sulfoxide (MetSO)	105.2	11.91–398.6	138.6	61.54–302.3	0.1855
5-hydroxyindoleacetic acid (5-HIAA)	2776	1149–5515	2397	936.5–5157	0.9153
Glutamic acid (Glu)	7906	1927–27132	6161	2122–24891	**0.0027**

4. CONCLUSIONS

This study reported significant changes in urinary and serum metabolites following repeated blast exposure in military personnel. The differences between pre- and post-blast metabolite levels suggested changes in brain chemistry following repeated

blast exposure that have not previously been reported. Specifically, urinary levels of HVA, Glu, and LA were significantly different in military personnel during breaching exercises. Furthermore, the presentation of different metabolites in urine and serum suggested a dynamic temporal profile that may be used to characterize brain injuries at different time points following injury. The metabolic biomarker panel evaluated here may offer clinicians with new diagnostic and prognostic tools to assess and characterize blast-related brain injuries. Larger clinical studies into these metabolites may extend the generalizability of the findings of this study.

REFERENCES

1. M. Lindberg, S. Sloley, B. Ivins, D. Marion, E.M. Martin, Military TBI—What civilian primary care providers should know, J. Family Med. Prim. Care 10 (2021) 4391-4397. doi: 10.4103/jfmpc.jfmpc_98_21.

2. W. Carr, J.R. Stone, T. Walilko, L.A. Young, T.L. Snook, M.E. Paggi, J.W. Tsao, C.J. Jankosky, R.V. Parish, S.T. Ahlers, Repeated low-level blast exposure: A descriptive human subjects study, Mil. Med. 181 (2016) 28-39. doi: 10.7205/MILMED-D-15-00137.

3. T. McAllister, M. McCrea, Long-term cognitive and neuropsychiatric consequences of repetitive concussion and head-impact exposure, J. Athl. Train. 5 (2017) 309-317. doi: 10.4085/1062-6050-52.1.14.

4. D.L. Dickstein, R.D. Gasperi, M.A. Sosa, G. Perez-Garcia, J.A. Short, H. Sosa, G. Perez, A.E. Knesaurek, A. Knutsen, D.L. Pham, L. Soleimani, B.D. Jordan, W.A. Gordon, B.N. Delman, G. Shumyatsky, P. Shahim, S.T. DeKosky, J.R. Stone, E. Peskind, K. Blennow, H. Zetterberg, S.A. Chance, M. Torso, L. Kostakoglu, M. Sano, P.R. Hof, S.T. Ahlers, S. Gandy, G.A. Elder, Brain and blood biomarkers of tauopathy and neuronal injury in humans and rats with neurobehavioral syndromes following blast exposure, Mol. Psychiatry 26 (2021) 5940-5954. doi: 10.1038/s41380-020-0674-z.

5. X. Xu, M. Cowan, F. Beraldo, A. Schranz, P. McCunn, N. Geremia, Z. Brown, M. Patel, K.L. Nygard, R. Khazaee, L. Lu, X. Liu, M.J. Strong, G.A. Dekaban, R.

Menon, R. Bartha, M. Daley, H. Mao, V. Prado, M.A. Prado, L. Saksida, T. Bussey, A. Brown, Repetitive mild traumatic brain injury in mice triggers a slowly developing cascade of long-term and persistent behavioral deficits and pathological changes, Acta. Neuropathol. Commun. 9:60 (2021). doi: 10.1186/s40478-021-01161-2.

6. S.M. Slobounov, A. Walter, H.C. Breiter, D.C. Zhu, X. Bai, T. Bream, P. Seidenberg, X. Mao, B. Johnson, T.M. Talavage, The effect of repetitive subconcussive collisions on brain integrity in collegiate football players over a single football season: A multi-modal neuroimaging study, Neuroimage Clin. 14 (2017) 708-718. doi: 10.1016/j.nicl.2017.03.006.

7. G.A. Elder, M.E. Ehrlich, S. Gandy, Relationship of traumatic brain injury to chronic mental health problems and dementia in military veterans, Neurosci. Lett. 707 (2019). doi: 10.1016/j.neulet.2019.134294.

8. A. Loignon, M.C. Ouellet, G. Belleville, A systematic review and meta-analysis on PTSD following TBI among military/veteran and vivilian populations, J. Head Trauma Rehabil. 35 (2020) E21-E35. doi: 10.1097/HTR.0000000000000514.

9. W. Carr, E. Polejaeva, A. Grome, B. Crandall, C. LaValle, S.E. Eonta, L.A. Young, Relation of repeated low-level blast exposure with symptomology similar to concussion, J. Head Trauma Rehabil. 30 (2015) 47–55. doi: 10.1097/HTR.0000000000000064.

10. G. Ling, J.M. Ecklund, F.A. Bandak, Brain injury from explosive blast: description and clinical management, in P. Vinken, G. Bruyn (Eds.) Handbook of Clinical Neurology, Elsevier, (2015) 173-180.

11. M. Edalatfar, S. Piri, M. Mehrabinejad, M. Mousave, S. Meknakhah, M. Fattahi, Z. Kavyani, A. Hajighadery, M. Kaveh, A. Aryannejad, M. Ghafouri, E. Jamshidi, M. Mehdi, A. Bari, M. Alhoseini, Biofluid biomarkers in traumatic brain injury: A systematic scoping review, Neurocrit. Care, 35 (2021) 559–572. doi: 10.1007/s12028-020-01173-1.

12. D.V. Agoston, A. Shutes-David, E.R. Peskind, Biofluid biomarkers of traumatic brain injury, Brain Inj. 31 (2017) 1195–1203. doi: 10.1080/02699052.2017.1357836.

13. L. Schiff, N. Hadker, S. Weiser, C. Rausch, A literature review of the feasibility of glial fibrillary acidic protein as a biomarker for stroke and traumatic brain injury. Mol. Diagn. Ther. 16 (2012) 79–92. doi: 10.1007/BF03256432.

14. A. Rodríguez-Rodríguez, J.J. Egea-Guerrero, A. León-Justel, E. Gordillo, J. Revuelto-Rey, A. Vilches-Arenas, A. Carrillo-Vico, J.M. Dominguez, F.M.

Cabezas, J.M. Guerrero, Role of S100B protein in urine and serum as an early predictor of mortality after severe traumatic brain injury in adults, Clin. Chim. Acta. 414 (2012) 228-233. doi: 10.1016/j.cca.2012.09.025.

15. J.R. Kulbe, J.W. Geddes, Current status of fluid biomarkers in mild traumatic brain injury, Exp. Neurol. 275 (2016) 334–352. doi: 10.1016/j.expneurol.2015.05.004.

16. C.B. Jeter, G.W. Hergenroeder, M.J. Hylin, J.B. Redell, A.N. Moore, and P.K. Dash, Biomarkers for the diagnosis and prognosis of mild traumatic brain injury/concussion, J. Neurotrauma 30 (2013) 657–670. doi: 10.1089/neu.2012.2439.

17. R. Vorn, R. Naunheim, C. Lai, C. Wagner, J.M. Gill. Elevated axonal protein markers following repetitive blast exposure in military personnel, Front. Neurosci. 16 (2022) 853616. doi: 10.3389/fnins.2022.853616.

18. M. An, Y. Gao, Urinary biomarkers of brain diseases, Genom. Proteom. Bioinform. 13 (2015) 345-354. doi: 10.1016/j.gpb.2015.08.005

19. A. Sigler, X. He, M. Bose, A. Cristea, W. Liu, P. Ki-Souk Nam, D. James, C. Burton, H. Shi, Simultaneous determination of eight urinary metabolites by HPLC- MS/MS for noninvasive assessment of traumatic brain injury, 31 (2020) 1910- 1917. doi: 10.1021/jasms.0c00181.

20. A. J. Baker, R. J. Moulton, V. H. MacMillan, and P. M. Shedden, Excitatory amino acids in cerebrospinal fluid following traumatic brain injury in humans, J. Neurosurg. 79 (1993) 369-372. doi: 10.1089/neu.2018.5919.

21. R.O. Bahado-Singh, S. Graham, B. Han, O. Turkoglu, J. Ziaeh, R. Mandal, A. Er., D.S. Wishart, P. Stahel, Serum metabolomic markers for traumatic brain injury: a mouse model, Metabolomics 12 (2016) 100. doi: 10.1007/s11306-016-1044-3.

22. I. Jalloh, A. Helmy, D.J. Howe, R.J. Shannon, P. Grice, A. Mason, C.N. Gallagher, M.P. Murphy, J.D. Pickard, D.K. Menon, K.L. Carpenter, Comparison of oxidative lactate metabolism in traumatically injured brain and control brain, J. Neurotrauma35 (2018) 25–35. doi: 10.1089/neu.2017.5459.

23. T.S. Anthonymuthu, E.M. Kenny, A.M. Lamade, V.E. Kagan, H. Bayır, Oxidized phospholipid signaling in traumatic brain injury, Free Radic. Biol. Med 124 (2018) 493-503. doi: 10.1016/j.freeradbiomed.2018.06.031.

24. H. Song, J. Cui, A. Simonyi, C.E. Johnson, G.K. Hubler, R.G. DePalma, Z. Gu, Linking blast physics to biological outcomes in mild traumatic brain injury:

Narrative review and preliminary report of an open-field blast model, Behav. Brain Res. 340 (2018) 147-158. doi: 10.1016/j.bbr.2016.08.037.

25. A.D. Corte, G. Chitarrini, I.M. Di Gangi, D. Masuero, E. Soini, F. Mattivi, U. Vrhovsek, A rapid LC–MS/MS method for quantitative profiling of fatty acids, sterols, glycerolipids, glycerophospholipids and sphingolipids in grapes, Talanta 40 (2015) 52-61. doi: 10.1016/j.talanta.2015.03.003.

26. C. Burton, H. Shi, Y. Ma, Normalization of urinary pteridines by urine specific gravity for early cancer detection, Clin. Chim. Acta 435 (2014) 42–47. doi: 10.1016/j.cca.2014.04.022.

27. J. Ozga, J. Povroznik, E. Engler-Chiurazzi, C. Haar, Executive (dys)function after traumatic brain injury: special considerations for behavioral pharmacology. Behav. Pharmacol. 7 (2018) 617-637. doi: 10.1097/FBP.0000000000000430.

28. A. Wagner, A. Kline, J. Sokoloski, R. Zafonte, E. Capulong, C. Dixon, Intervention with environmental enrichment after experimental brain trauma enhances cognitive recovery in male but not female rats, Neurosci. Letters, 334 (2002) 165-168. doi: 10.1016/S0304-3940(02)01103-5.

29. C.J. Vecht, T.C.A.M. van Woerkom, A.W. Teelken, J.M. Minderhoud. Homovanillic acid and 5-hydroxyindoleacetic acid cerebrospinal fluid level, a study with and without probenecid administration of their relationship to the state of consciousness after heard injury, Arch Neurol 32 (1975) 792-797.

30. S.R. Bareggi, M. Porta, A. Selenati, B. Assael, G. Calderini, M. Collice, M. Rossanda, P.L. Morselli, Homovanillic acid and 5-hydroxyindole-acetic acid in the CSF of patients after a severe head injury I. Lumbar CSF concentrations in chronic brain post-traumatic syndromes, Eur. Neurol. 13 (1975) 528-544.

31. E.A. Bykowski, J.N. Petersson, S. Dukelow, C. Ho, C.T. Delbert, T. Montina, G. Metz, Urinary metabolomic signatures as indicators of injury severity following traumatic brain injury: A pilot study, IBRO Rep 11 (2021) 200-206. doi: 10.1016/j.ibneur.2021.10.003.

32. S. Mondello, K. Schmid, R. Berger, F. Kobeissy, D. Italiano, A. Jeromin, R. Hayes, F. Tortella, A. Buki, The challenge of mild traumatic brain injury: Role of biochemical markers in diagnosis of brain damage, Med. Res. Reviews 34 (2014) 503-531. doi: 10.1002/med.21295.

33. R.M. Guerriero, C.C. Giza, A. Rotenberg, Glutamate and GABA imbalance following traumatic brain injury, Curr. Neurol. Neurosci. Rep. 15 (2015) 27. doi: 10.1007/s11910-015-0545-1.

34. M. Hennebelle, Z. Zhang, A. Metherel, A. Kitson, Y. Otoki, C. Richardson, J. Yang, K. Lee, B. Hammock, L. Zhang, R. Bazinet, A. Taha, Linoleic acid participates in the response to ischemic brain injury through oxidized metabolites that regulate neurotransmission. Sci. Rep. 7 (2017) 4342. doi: 10.1038/s41598-017-029114-7.

35. J. Deutsch, S.I. Rapoport, A.D. Purdon, Relation between free fatty acid and acyl-CoA concentrations in rat brain following decapitation, Neurochem Res 22 (1997) 759–765.

36. M. Strokin, M. Sergeeva, G. Reiser, Docosahexaenoic acid and arachidonic acid release in rat brain astrocytes is mediated by two separate isoforms of phospholipase A2 and is differently regulated by cyclic AMP and Ca2+. British journal of pharmacology 139 (2003) 1014–1022. doi:10.1038/sj.bjp.0705326.

37. T.L. Blasbalg, J.R. Hibbeln, C.E. Ramsden, S.F. Majchrzak, R.R. Rawlings, Changes in consumption of omega-3 and omega-6 fatty acids in the United States during the 20th century. Am J Clin Nutr 93 (2011) 950–962. doi:10.3945/ajcn.110.006643.

38. M. Hajiaghamemar, T. Kilbaugh, K.B. Arbogast, C.L. Master, S.S. Margulies, Using serum amino acids to predict traumatic brain injury: A systematic approach to utilize multiple biomarkers, Int. J. Mol. Sci. 21 (2020) 1786. doi: 10.3390/ijms21051786.

39. I. L. Simone, M. Ruggieri, R. Tortelli, E. Ceci, E. D'Errico, A. Leo, S. Zoccolella, M. Mastrapasqua, R. Capozzo, P. Livrea, G. Logroscino, Serum N-acetylaspartate level in amyotrophic lateral sclerosis, archives neurol. 68 (2011) 1308-1312. doi: 10.1001/archneurol.2011.217.

40. E.E. Bernarroch, N-acetylaspartate and N-acetylaspartylglutamate: Neurobiology and clinical significance, Neurology 70 (2008) 1353-1357. doi: 10.1212/01.wnl.0000311267.63292.6c.

41. F. Pifferi, B. Laurent, M. Plourde, Lipid transport and metabolism at the blood-brain interface: Implications in health and disease, Front. Physiol. 12 (2021) 645646. doi: 10.3389/fphys.2021.645646.

III. DEVELOPMENT OF A SINGLE CELL ICP-MS METHOD TO STUDY LEGIONELLA PNEUMOPHILIA TREATMENT WITH COPPER IN DRINKING WATER

Austin Sigler,[1,#] Lei Xu[2,#] Anna Chernatynskaya,[2] Lindsey Rasmussen,[1] Jingrang Lu,[3] Endalkachew Sahle-Demessie,[3] David Westenberg,[4] Hu Yang,[2,*] Honglan Shi,[1,*]

[1]Department of Chemistry and Center for Research in Energy and Environment, Missouri University of Science and Technology, Rolla, MO 65409, USA

[2]Linda and Bipin Doshi Department of Chemical and Biochemical Engineering, Missouri University of Science and Technology, Rolla, MO, 65409, USA

[3]US Environmental Protection Agency, Office of Research and Development, Cincinnati, OH, USA

[4]Department of Biological Sciences, Missouri University of Science and Technology Rolla, MO, 65409, USA

# These authors contribute equally to this work.

*** Corresponding authors:**

Honglan Shi
Ph: 573-341-4433
Email:
honglan@mst.edu
ORCID: 0000-
0002-0801-5683

Hu Yang
Ph: 573-341-4854
Email: huyang@mst.edu

ABSTRACT

Legionella pneumophila is a persistent opportunistic pathogen that poses a significant threat to domestic water systems. Previous studies suggest that copper (Cu) is

an effective antimicrobial in water systems. A rapid and sensitive quantification method is desired to optimize the conditions of L. pneumophila treatment by Cu and to better understand the interaction mechanisms between Cu and cells. In this study, we developed a highly sensitive single cell (SC) -ICP-MS method to monitor L. pneumophila cell concentration and track their uptake of Cu. The SC-ICP-MS method showed excellent sensitivity (with a cell concentration detection limit of 1000 cells/mL), accuracy (good agreement with conventional hemocytometry method), and precision (relative standard deviation <15%) in drinking water matrix. The Cu treatment results indicated that the total L. pneumophila cell concentration, Cu mass per cell, CFU counting, and Cu concentration in supernatant all exhibited a dose-dependent trend, with 800 −1200 μg/L reaching high disinfection rates in drinking water. The investigation of percentages of viable and culturable (VC), viable but nonculturable (VBNC), nonviable but has intact shape (NVBI), and nonviable and lysed (NVL) cells proved that Cu treatment can change VC cell to NVL cell effectively without forming NVBI cell, but Cu cannot affect the ratio of VBNC cell significantly. There is no obvious proportional correlation between Cu contact time and disinfection efficiency. The L. pneumophila cell possibly developed a bactericide resistant mechanism with the prolonged Cu exposure, or a portion of the L. pneumophila population, VBNC cells, never took up Cu during the treatment. This is the first quantification study on the interactions of Cu and L. pneumophila in drinking water using SC-ICP-MS.

Keywords: Single cell-ICP-MS, Legionella pneumophila, copper (Cu), antimicrobial resistance, water treatment, magnesium (Mg)

1. INTRODUCTION

Legionella pneumophila is an opportunistic pathogen that is responsible for cases of Legionnaires' disease, severe and potentially fatal pneumonia. According to the World Health Organization (WHO), the disease affects approximately 10,000 to 18,000 people annually in Europe alone, with a case-fatality rate ranging from 5% to 30% (WHO, 2019). Outbreaks of Legionnaires' disease have been linked to a variety of sources, including cooling towers, hot tubs, and showerheads. However, the presence of L. pneumophila in drinking water systems is a major public health concern, as it can cause disease outbreaks and result in widespread exposure to contaminated water. In the United States, Legionella accounted for no less than ten waterborne disease outbreaks from 2011 to 2014 (1-3) and resulted in over 500 cases and 11 deaths from 2019 to 2022 (). Furthermore, the annual crude incidence rate of Legionnaires' disease per million residences in the United States has substantially increased from 4.2 in 2000 to 18.9 in 2015 (4). Therefore, it is critical to control the growth of L. pneumophila in the drinking water systems.

Copper (Cu) is a commonly used chemical treatment to control L. pneumophila and other microorganisms (5-7). Cu ions have been shown to have a bactericidal effect on L. pneumophila, with several studies demonstrating a significant reduction in the number of L. pneumophila cells in water samples after exposure to Cu. For example, Lin et al. found that exposure to 4400 μg/L of Cu resulted in a 4 log (99.99%) reduction of L. pneumophila in one hour (8). Song et al. reported that L. pneumophila in the early stationary growth phase was reduced by up to 4 logs in 6 h after dosing 600 μg/L Cu (9).

Cu has also been found to be an effective treatment for controlling other waterborne pathogens, such as Staphylococcus aureus, Escherichia coli, and Enterococcus faecalis (10). However, evaluating the Cu dose effect in drinking water systems remains challenging because water chemistry can strongly affect it (9). Up to now, the optimal conditions for using Cu to treat drinking water have not been well established and the interaction mechanisms between Cu and cells is still not fully understood. The efficacy of Cu treatment depends on several factors, including the type of Cu species used, the concentration of Cu in water, the contact time of Cu, the pH of water, and the presence of other chemicals, such as phosphate and chloride (9). To better understand the impact of these factors and the mechanism of Cu-L. pneumophila interaction, it is essential to have a rapid and sensitive analytical method.

The primary analytical techniques used for evaluating the efficiency of Cu treatment for L. pneumophila are inductively coupled plasma-optical emission spectroscopy (ICP-OES), inductively coupled plasma mass spectrometry (ICP-MS), etc (9, 11, 12). Conventional ICP-MS analysis is limited to measurements of the average amount of metal per cell in a cell population after laborious acid digestion (13-15). It cannot provide intracellular concentrations for individual cells needed to construct mass distributions across a heterogeneous population. Single cell (SC)-ICP-MS is a cutting-edge analytical technique that allows the quantification of elemental content in an individual cell and the distribution in the cell population. It has been increasingly used for studying interactions of metal containing materials, including nanoparticles and bactericides, with algae, yeast, and other microorganisms (15-24), as well as human cancer cells (23, 25, 26). SC-ICP-MS has key advantages: (1) It is very sensitive,

allowing intracellular measurement of metal down to attogram (ag) per cell at single cell level; (2) it can monitor Cu in cells directly without acid digestion as needed by conventional ICP-MS and ICP-OES; (3) it provides the distribution of the metal content within a cell population rapidly, allowing for the discrimination of differences due to cell heterogeneity; (4) It can analyze a large number of individual cells in a short amount of time, allowing for high throughput analysis. The SC-ICP-MS analysis employs time-resolved techniques utilizing a low flow rate high- efficiency nebulizer. The principle of the technique has been established (16, 27). SC-ICP- MS is expected to have high potential for the investigation of L. pneumophila treatment and interaction mechanism with Cu and other metallic bactericides. However, a SC-ICP- MS method has not been developed for this type of analysis. In response, we developed a highly sensitive and rapid SC-ICP-MS method for quantifying Cu uptake by L. pneumophila at the single cell level. We have applied this SC-ICP-MS method to quantitatively evaluate the treatment efficiency by different Cu concentrations and contact times in a drinking water system. The technique is expected to lead to applications for studying the Cu and L. pneumophila interaction mechanism.

2. MATERIALS AND METHODS

2.1. MATERIALS

Trace-metal-grade concentrated nitric acid (HNO3, 67−70%), copper sulfate (CuSO4·5H2O, > 99.9%), sodium hydroxide (NaOH, > 99.9%), sodium chloride (NaCl,

> 99%), isopropyl alcohol (> 99.9%) were all purchased from Fisher Scientific (Pittsburgh, PA, United States). Dissolved Cu, magnesium (Mg), and Bismuth (Bi) standard solutions (10 mg/L in 2% HNO3) were purchased from High-Purity Standards (Charleston, SC, United States). Supplies for bacterial culture were purchased from Sigma-Aldrich, Inc., St. Louis, MO in United States (potassium hydroxide, activated charcoal, agar, L-cysteine) and Thermo Fisher Scientific Waltham, MA in United States (yeast extract, ACES buffer, alpha-ketoglutarate, thymidine). Ferric nitrate was purchased from MP Biomedicals (Solon, OH, USA). Ultrapure water (18.2 MΩ·cm) was prepared using a Millipore water purification system (Millipore, Billerica, MA, USA).

2.2. BACTERIAL STRAINS AND CULTURE CONCENTRATIONS

L. pneumophila strain Lp02 was used in this study as previously described (28). The bacteria were grown on buffered charcoal yeast extract (BCYE) agar plates (supplemented with 0.4 mg/ml L-cysteine 0.1 mg/ml thymidine, 0.135 mg/ml ferric nitrate) for 2−4 days at 37 ℃. Several single colonies were transferred to a 16 mm × 150 mm test tube with 5 mL of BYE broth (N-(2-acetamido)-2-aminoethansulfonic acid-buffered yeast extract broth supplemented with 0.4 mg/mL L-cysteine, 0.1 mg/mL thymidine, and 0.135 mg/mL ferric nitrate). The initial optical density of the bacterial culture at a wavelength of 600 nm (OD600) was 0.2. Cells were grown for 16 h (early stationary phase) at 37 °C with constant shaking at 200 rpm. After incubation, cells were pelleted by centrifuging at 5,000 g for 5 min, and then the supernatant was discarded. Cells were washed twice with 5 ml of 0.9% saline solution. The cell pellet was resuspended in 5 mL of filter-sterilized ultrapure water and diluted to obtain OD600 =0.2.

The bacterial cell suspension was further diluted to obtain approximately OD600 =0.02 to perform cell count using a hemocytometer for total L. pneumophila cell concentration. The cell count was determined according to standard protocol using a Leica model ICC50W microscope with phase contrast optics at 400 times magnification. After determining the cell concentration based on the hemocytometer calculations, bacterial cells were diluted with sterile water to a final concentration of cells of 3 × 106 cells/mL for the corresponding treatment experiment.

2.3. DRINKING WATER SAMPLE COLLECTION AND WATER PARAMETERS

The drinking water from a local municipal utility in Missouri was collected and used for these experiments. The drinking water was allowed to run from the faucet for about 5 mins, then collected in pre-cleaned glass containers. The sample was left at room temperature for a few days until no disinfectant (chlorine) residue was left in the water. The water was then filtered through a 0.22 μm nylon membrane filter to remove any particulates and microorganism, if present. The pH and dissolved organic carbon (DOC) of water sample were measured and listed in Table 1. By following standard procedure, DOC was measured using a Shimadzu Model TOC-L TOC analyzer (Shimadzu, Overland Park, KS, USA). The water was also tested for native Mg and Cu concentrations by conventional ICP-MS method using a PerkinElmer NexION 2000P ICP-MS (Shelton, CT, USA) after appropriate dilution using 1% HNO3. The dissolved Mg and Cu standards in concentration range from 0.01 to 500 μg/L were applied to establish calibration curves. Bi (0.5 μg/L) was used as the internal standard added online

during the ICP-MS analysis. The reagent blank, duplicate, and spiked samples were also monitored for quality assurance. The concentrations are shown in Table 1.

Table 1. Drinking water sample important parameters

Sample Parameter	Value
pH	7.10
Dissolved organic carbon (DOC)	3.81 mg/L
Total dissolved solids	243.0 mg/L
Cu concentration	120.0 µg/L
Mg concentration	32.2 mg/L

2.4. CU TREATMENT OF L. PNEUMOPHILIA IN DRINKING WATER

A Cu stock solution of 100 mg/L was prepared using CuSO4·5H2O and adjusted pH = 4.0 ± 0.05 to maintain Cu solubility. The intermediate/working solution of Cu 10 mg/L was freshly diluted using ultrapure water right before each treatment experiment. The pH = 7 ± 0.05 was adjusted using 0.1 N potassium hydroxide or 0.2 N nitric acid and solution was sterilized using 0.22 µm nylon membrane filter. Ultrapure water and 0.9% saline solution were tested by ICP-MS for blank background levels of Cu and Mg and then sterilized by using a 0.22 µm filter system.

The treatments were prepared by using 3 × 106 L. pneumophila cells/mL in 5 mL of water with the corresponding addition of Cu stock solution (10 mg/L) to achieve Cu concentrations at 0 (control), 100, 400, 800, and 1200 µg/L. Note that in native drinking water, 120 µg/L of Cu was present in addition to the spiked concentration. The bacterial

cell suspensions in the water were incubated for 4 h at 37 °C with constant shaking at 200 rpm. The Cu concentration of 800 μg/L was selected for measuring the impact of contact time (0.08, 0.5, 2, 4, 8, and 24 h).

After treatment, cells were transferred to 15 mL of conical tubes and cells were pelleted by centrifuging for 5 min at 5,000 g. The supernatant was removed by gentle pipetting to avoid loss of cells. The supernatants of selected samples were collected for Cu analysis by conventional ICP-MS. The cell pellet was washed and then resuspended in 3 mL of ultrapure water. An aliquot of cell suspension was used for SC-ICP-MS analyses for Cu uptake by L. pneumophila through monitoring 63Cu and total cell concentration through monitoring 24Mg. The total cell (TC) concentration measured through 24Mg SC-ICP-MS includes viable and culturable (VC), viable but nonculturable (VBNC), and nonviable (NV or died) cells with intact cellular shape (NVBI). Only nonviable and lysed (NVL) cell cannot be detected. The detailed relationship between TC, VC, VBNC, NV, NVBI, and NVL is shown in Figure S1. An aliquot of cell suspension was used for counting colony-forming units (CFU) to determine the VC cell concentration after the Cu treatment.

2.5. SINGLE CELL ICP-MS METHODS

A PerkinElmer NexION 2000P ICP-MS equipped with a single cell sample introduction system and controlled by Syngistix for ICP-MS software (PerkinElmer, Shelton, CT, USA) was employed for SC-ICP-MS analysis. The detailed information about PerkinElmer SC-ICP-MS sample introduction system (nebulizer, spray chamber, and injector) is shown in Table 2. Manual sample introduction was used for each sample

at a flow rate of 14 µL/min following a 3 min rinse cycle with 0.1% nitric acid and ultrapure water. Nebulizer and make-up gas flows were optimized daily, but generally proceeded at 0.32 L/min and 0.70 L/min, respectively. The scan time was set to 100 s, with a dwell time at 50 µs. Prior to each experiment, the spray chamber was cleaned thoroughly with 99.9% isopropyl alcohol followed by ultrapure water.

2.6. CFU COUNTS FOR VIABLE AND CULTURABLE L. PNEUMOPHILIA CELL CONCENTRATION DETERMINATION

An aliquot of 0.1 mL from each replicate of treated sample was transferred to a sterile microcentrifuge tube preloaded with 0.09% saline. Serial dilutions of (1:100−1:1000) were prepared and 0.1 mL was transferred onto BCYE agar plate. After 72 h of incubation, colonies were enumerated manually.

2.7. FLOW CYTOMETRY ANALYSIS TO DETECT CELL VIABILITY

L. pneumophila cells viability was assessed by a BD AccuriTM C6 Plus Flow Cytometer (BD Biosciences, Becton-Dickinson, Franklin Lakes, NJ) with BD Accuri C6 Plus software and Live/Dead BacLight Bacterial Viability kit (SYTO® 9 green fluorescent nucleic acid stain and propidium iodide red fluorescent nucleic acid stain) following the manufacturer's instruction. L. pneumophila cells were treated with different concentrations of Cu (0, 100, 400, 800, and 1200 µg/L) for 4 h in drinking water at 37 oC, pH 7. After the treatment, cells were spin down and resuspended in ultrapure water for flow cytometry analysis.

2.8. STATISTICAL ANALYSIS

Data analysis was performed using the statistical software Microsoft Excel 365 (Microsoft Corp.). Data are representative of three independent experiments and expressed as mean ± SD (n = 3, technical replicates). Figures were drawn by OriginPro 2021 (Origin Lab, United States). The statistical analysis was performed by IBM SPSS Statistics 27.0.1 using one-way ANOVA with Duncan's post-hoc test. An outcome was considered statistically significant if a p-value of < 0.05 was obtained.

3. RESULTS AND DISCUSSION

3.1. SINGLE CELL ICP-MS METHOD DEVELOPMENT AND PERFORMANCE

Transport efficiency (TE) was measured by using the L. pneumophila cells by monitoring the intrinsic metal 24Mg due to its high concentration in cells and relatively low background, using the same procedure as our previous method for the SC-ICP-MS method for algae cells (17). A representative histogram of intracellular Mg mass distribution in L. pneumophila cell is shown in Figure 1. The histograms of the suspensions were Gaussian shape except for some noise in the very low signal intensities, which were eliminated from the calculations. The TE was ranged from 44% to 56% from day to day (measured daily for each experiment). This noise is to be expected as cell pieces can be generated during the log phase of cell growth.

The cell concentrations in cell suspension were measured by SC-ICP-MS and calculated by Syngistix software using the measured TE and the measured counts per second for intrinsic Mg in each suspension. All the method conditions were optimized to

the highest TE and reproducibility while ensuring cell integrity through the sample introduction system. The optimized method parameters are tabulated in Table 2.

To evaluate the Cu mass in each cell, external calibration curve with dissolved Cu standard solutions (0, 0.1, 1, 5, and 10 μg/L) was established.

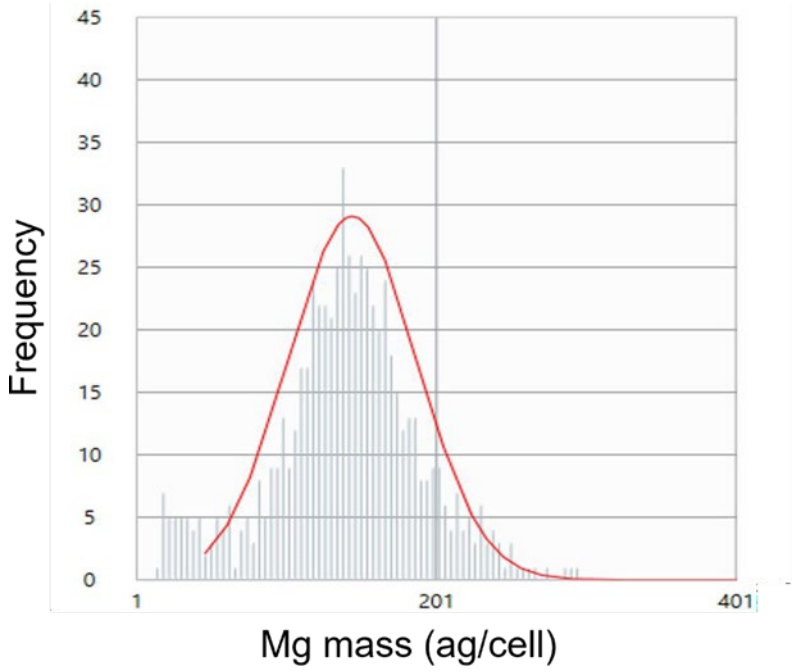

Figure 1. A representative histogram of ^{24}Mg SC-ICP-MS from a *L. pneumophila* cell suspension.

The detection limit was calculated to be 38 ag Cu/cell following the equation below (1):

$$DL = \frac{3\sigma}{slope\ of\ calibration\ curve} \quad (1)$$

where σ is the standard deviation of the blank, and DL is the mass detection limit (ag Cu/cell).

Table 2. Optimized SC-ICP-MS parameters.

Parameter	Optimized Value
Manual Sampling Flow Rate	14 µL/min
Nebulizer	Meinhard TRP-90-A0.05
Spray Chamber	Asperon Single-Cell
Injector	Quartz. 2.0 mm id
RF Power	1600 W
Nebulizer gas flow rate*	0.32 L/min
AMS makeup gas flow rate	0.70 L/min
Analytes	24Mg and 63Cu
Transport efficiency (TE)*	44%−56%
Sample analysis time	100 s
Dwell time	50 s

Due to the nature of L. pneumophila cells which tend to aggregate and attach to the wall or bottom of the container (29), verifying the linearity of cell suspension dilutions was necessary. As such, different dilutions of a suspension were made from 7.2× 105 cells/mL to 1000 cells/mL and the cell concentrations measured exhibited excellent linearity (Figure 2).

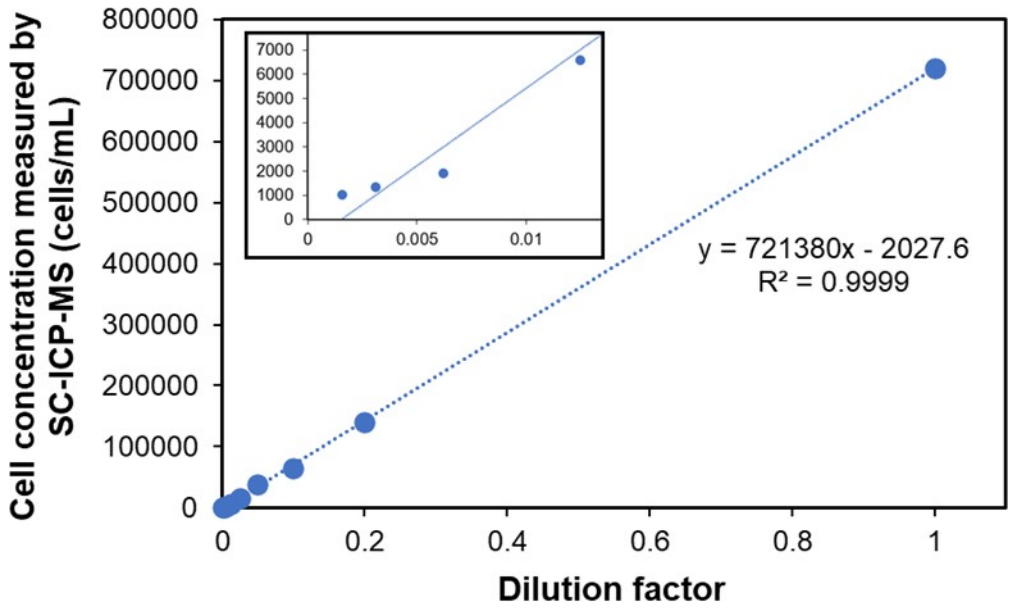

Figure 2. SC-ICP-MS results from different dilutions of a stock cell suspension by measuring 24Mg. The cell concentration in stock suspension is 7.2 × 105 cell/mL counted by hemocytometer.

Finally, to confirm the agreement between SC-ICP-MS and conventional hemocytometry counting, cell concentrations were determined using both the hemocytometer and SC-ICP-MS in three replicates of cell suspensions. The cell concentrations from both the hemocytometer and SC-ICP-MS gave good consistency. The SC-ICP-MS measured cell concentration were 2.7 × 105, 2.9 × 105, and 2.7 × 105 cells/mL, with a RSD of 4.2%. The cell concentration obtained by hemocytometer count were 2.8 × 105, 2.7 × 105, and 2.3 × 105 cells/mL, with a RSD of 10.2%. The SC-ICP-MS measurement is not only much faster than the conventional cell count, but it also has improved reproducibility.

3.2. CU CONCENTRATION IMPACT ON LEGIONELLA PNEUMOPHILIA TREATMENT EFFECTIVENESS

The histograms of Cu mass distribution in cell population after treatments (4 h, 37°C) with different Cu concentrations in drinking water are shown in Figure 3. Compared with the control group (no Cu dose), the L. pneumophila cells exhibit obvious heterogenicity in Cu uptake, with the long tail observed after dosing Cu.

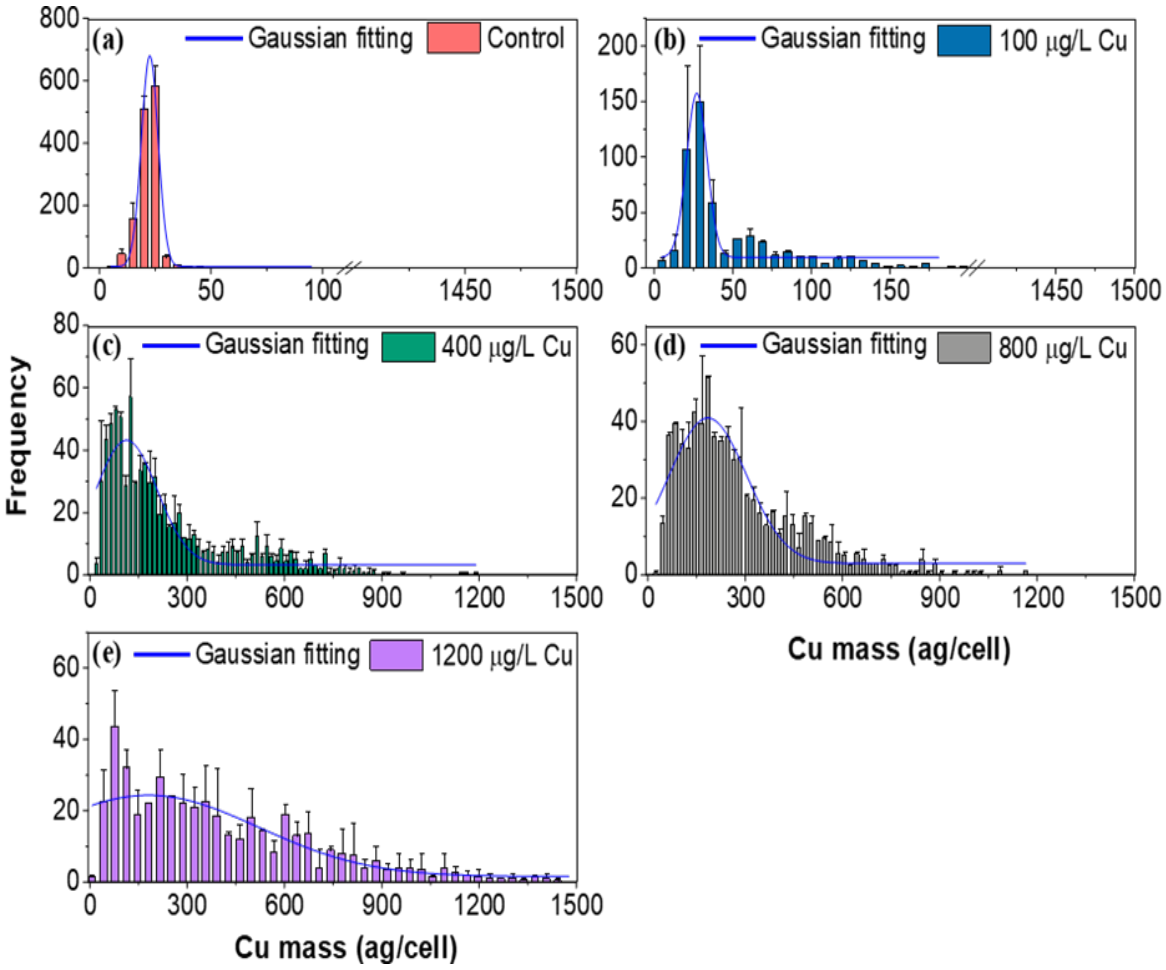

Figure 3. Histogram of Cu mass in individual L. pneumophila cell after treatments with different Cu concentrations (a for control; b for 100 µg/L Cu; c for 400 µg/L Cu; d for 800 µg/L Cu; e for 1200 µg/L Cu). The error bars in the SP-ICP-MS histograms represent standard deviation (n = 3).

The gradually right-shifted Gaussian fitting peak with the increase of Cu treatment concentration indicates the dose-dependent phenomenon of Cu uptake. It is worth noting that the Cu mass histogram detected in control group should be caused by cellular uptake of Cu ions from the original drinking water.

To further investigate the Cu concentration impact on L. pneumophila cell, the TC concentration and average Cu mass per cell were tested by SC-ICP-MS (Figures 4a and 4b). During the SC-ICP-MS analysis, 24Mg was monitored as an intrinsic metal in cells for TC concentration determination. As shown in Figure 4a, the TC concentration detected by SC-ICP-MS decreases significantly ($p < 0.05$) with increased Cu treatment concentration. When dosing with 800 μg/L and 1200 μg/L of Cu, the Cu disinfection rate reached similar high level, with cell losses of 41.3% and 46.9%, respectively, compared with the control group. As expected, the Cu mass in each cell increased with the increasing dosed Cu concentration (Figure 4b), indicating that the uptake of Cu by L. pneumophila caused a significant decrease of cell concentration. Notably, no significant difference ($p > 0.05$) of the Cu mass per cell in 800 μg/L Cu treatment group and the 1200 μg/L Cu treatment group), all close to 300 ag Cu/cell. This should be the reason why TC concentration in the 1200 μg/L Cu treated group was only slightly decreased compare with that from 800 μg/L Cu treated group. more importantly, it might be a potential indicator showing that in this drinking water chemistry situation, Cu mass of 300 ag/cell after dosing 800−1200 μg/L Cu can reach the highest disinfection efficacy. SC-ICP-MS method can rapidly detect intact TC concentration, but it cannot distinguish the cell state. To examine culturable L. pneumophila cell, CFU count was determined after 72 h incubation and the results are shown in Figure 4c. CFU counting results also

display a dose-dependent trend, which agreed well with TC concentration results. The 800 μg/L and 1200 μg/L of Cu treatments also have similarly high disinfection level (56% and 58%, respectively). Interestingly, the VC cell concentrations detected by this plate count method were lower than the TC detected by SC-ICP-MS method in all groups, including control group at similar level (23%±2%). This presumably due to the presence of VBNC L. pneumophila cells in the original cell culture or induced transformation to VBNC state during the 4 h experimental time, or possibly some died cells not lysed during this time.

In order to find out if the difference of TC detected by SC-ICP-MS and CFU count is due to VBNC cells or died but not lysed cells, the cell viability was determined by flow cytometer analysis.

The results in Figure 5 indicates that most the cells (94.5, 93.7, 93.6, and 92.8% for control, 100, 800, and 1200 μg/L Cu treatment, respectively) detected by SC-ICP-MS were viable cells. This confirmed that the more cells detected by SC-ICP- MS than the CFU count were VBNC L. pneumophila cells, i.e., TC≈VC+VBNC.

Putting all different experiment together, the changes of percentages of VC, VBNC, and NVL cells after different Cu concentration treatments are demonstrated in Figure 6. As expected, the VC cell's percentage decreased and the NVL cell's percentage increased as the increase of Cu concentration. Interestingly, there is no obvious change about the ratios of VBNC cell after different Cu concentration treatments. Based on these percentage profiles, it could be speculated that after 4 h treatment, Cu is able to disinfect the L. pneumophila and change its state from VC to NVL cell, showing an obvious dose-dependent tendency, but did not affect the ratio of VBNC cell much. This seems

indicating there are certain percentage L. pneumophila cells present as VBNC cells under this treatment condition.

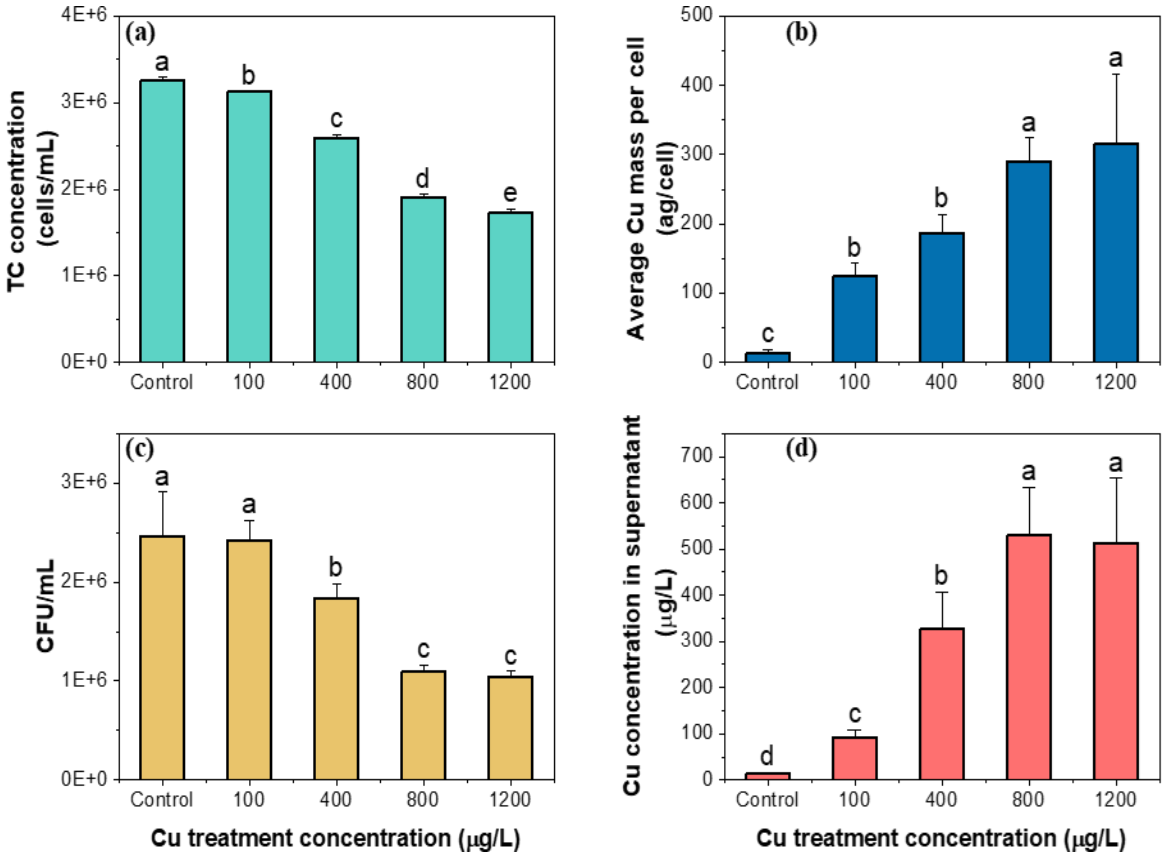

Figure 4. Cu treatment concentration (0−1200 μg/L) effect on L. pneumophila. (a) L. pneumophila TC concentration detected by SC-ICP-MS and percentage of TC intact cells after the treatment with different Cu concentrations; (b) average Cu mass per L. pneumophila cell after the treatment with different concentrations of Cu; (c) CFU/mL ofL. pneumophila cell and percentage of VC cell after the treatment with different Cu concentrations; (d) Cu concentration in supernatant after the treatment with different Cu concentrations. Data are representative of three independent experiments and expressed as mean ± SD (n = 3, technical replicates). The statistical analysis was performed by IBM SPSS Statistics 27.0.1 using one-way ANOVA with Duncan's post-hoc test. Different letters indicate significant differences between different treatments ($p < 0.05$).

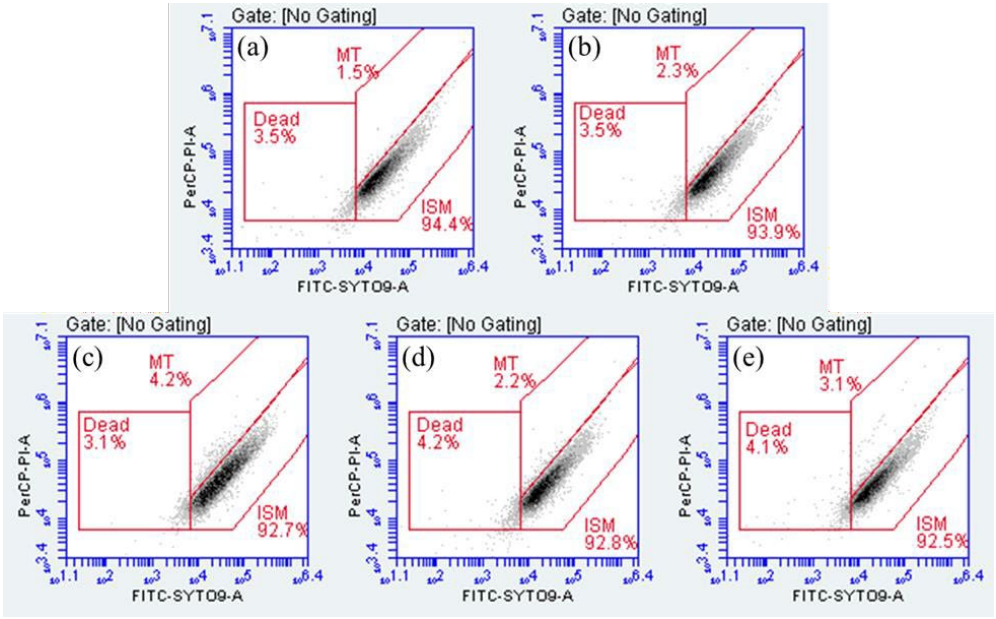

Figure 5. Cell viability determined by flow cytometry analysis of L. pneumophila treated with different concentrations of Cu in drinking water at a contact time of 4 h. (a) Control (drinking water without Cu addition), (b) 100 µg/L Cu, (c) 800 µg/L Cu, (d) 1200 µg/L Cu. ISM: intact slightly damaged membranes (viable cell). MT: mixed type membranes (damaged cell). ISM is the percentage of viable cells.

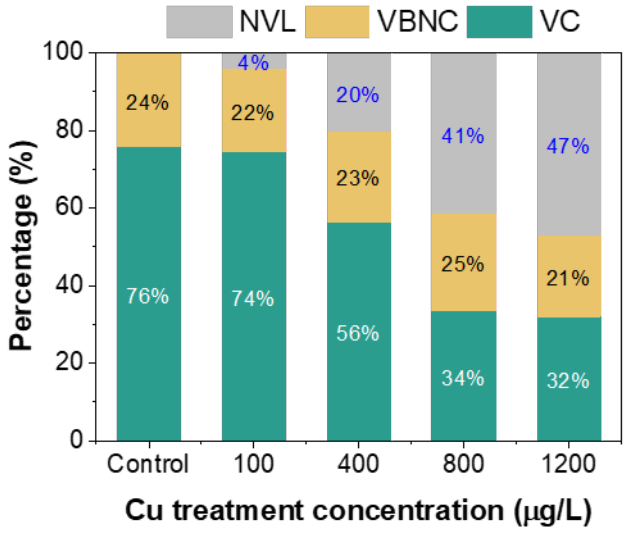

Figure 6. Percentages of VC (viable and culturable) cell, VBNC (viable but nonculturable) cell, and NVL (nonviable and lysed) cell revealed by SC-ICP-MS and CFU count methods after different concentrations of Cu treatment.

To find out why no significant increase of disinfection efficiency as increasing Cu to 1200 μg/L from 800 μg/L, the Cu concentrations in the cell culture supernatants (media after removing the cells) were detected by conventional ICP-MS and the results are shown in Figure 4d. It is clear that the dissolved Cu concentrations in the high Cu treatment samples are much lower than the dosed Cu concentrations, especially for the 1200 μg/L Cu group, which is about same as 800 μg/L Cu dosed one. The difference of lost Cu between 800 μg/L and 1200 μg/L treatment groups is about 417 μg/L, indicated no available Cu increased when higher Cu dosed. This may be due to the formation of Cu(OH)2 precipitation or other form, . This should be the main reason why the efficiency of 1200 μg/L treatment is similar with the 800 μg/L Cu treatment group.

Other studies have also shown that L. pneumophila concentration in drinking water exhibits a dose-dependent trend with Cu concentration. A study conducted by Emilie et al. investigated the impact of Cu concentration on L. pneumophila concentration in a hospital hot water system (12). The study found that as Cu concentration increased from 0.8 to 5 mg/L at pH 7.8, the log reduction in CFU counts of L. pneumophila cell increased from ~1 to ~5 after 672 h, demonstrating a clear dose-response relationship. Similarly, a study by Song et al. showed that with the increase of Cu concentration from 200 to 800 μg/L at pH 7, the log reduction of L. pneumophila increased from 1.5 to 4 after 6 h (9). However, Cu can also react with other components in drinking water, such as chloride and natural organic matter (NOM). After entering drinking water, dosed Cu can react with chloride and NOM in drinking water forming different complexes, such as CuCl and CuCl2, which have low solubility in water and are less available to organisms (9). Another factor that can influence the relationship between Cu and L. pneumophila

concentration in drinking water is the pH of the water. Recent studies found that the effectiveness of Cu in reducing L. pneumophila cell concentration was pH-dependent (8, 9), with the optimal pH being 7 when the dosed Cu concentration was 800 μg/L. Above this pH level, the antimicrobial effectiveness of Cu was reduced mainly due to the formation of Cu precipitation, as we observed in this study. For example, Song et al. treated tap water with 1000 μg/L Cu and monitored the soluble Cu content at different pH levels. After 20 mins, the soluble Cu was 87.2% of total Cu at pH 7.0 and decreased to 68.7% at pH 7.5, 41.4% at pH 8.0, and 23.7% at pH 8.5 (9).

Another important finding of our study is the alteration of the cell state during Cu treatment. The state transition from VC cell to NVL cell after Cu treatment should be associated with the "contact killing" process (31, 32). Cu ions can bind to cell membrane surface, and then disrupt the lipid bilayer and cause membrane damage, leading to increased permeability and loss of essential ions and molecules from the cell. This can ultimately result in the lysis or rupture of the cell membrane, leading to the elevated NVL cell percentage (33). Another toxicity mechanisms to inactivate L. pneumophila is the formation of reactive oxygen species (ROS). Cu ions can generate ROS in the presence of water or oxygen. ROS can cause damage to cellular components such as proteins, lipids, and DNA, leading to cellular dysfunction and death (34). Being unable to proliferate, L. pneumophila cell survive severe environmental conditions by entering the dormant state, i.e. VBNC cell state. Previous study reported that the Cu ion stressor can stimulate L. pneumophila to enter VBNC state (35). Once induced into VBNC state by Cu treatment, L. pneumophila cells usually tend to shrink and form a spheric shape, which may reduce their metabolic activity by decreasing specific surface area and further

reducing the exchange of Cu through their cell surface (36). In addition, previous studies found that the bacterial physiology also changes significantly after entering the VBNC state. These changes include a decrease in the transmission efficiency of nutrients and substances, a decrease in metabolic and respiratory activity, alterations in the composition of the cell wall and membrane, and changes in gene expression levels (37, 38). The decreased transmission efficiency, for example, hinders the Cu uptake and allows the L. pneumophila cells to survive with varying Cu concentration treatments. It should be noted that the VNBC L. pneumophila cells can be resuscitated by amoeba (39), hence further efforts are warranted to eradicate VNBC L. pneumophila in drinking water system.

3.3. CU TREATMENT CONTACT TIME IMPACT ON l. PNEUMOPHILIA TREATMENT EFFICACY

From the above experiment results, it was found that 800 μg/L Cu treatment was effective in disinfecting L. pneumophila cells for a treatment contact time of 4 h. Further tests were performed to evaluate the impact of different contact times on the efficiency of reducing L. pneumophila cell counts by treatment with 800 μg/L Cu. The contact times of 0.08, 0.5, 2, 4, 8, and 24 h were tested. The histograms at different contact times are shown in Figure 7. Even at ~0.08 h (5 min), unsymmetrical Cu mass histogram with a tail was observed, suggesting the rapid Cu uptake by L. pneumophila cells. Over time, the Gaussian fitting peak shifts to right side and frequency of cell with higher Cu mass elevates gradually, leading to a histogram with a high and long tail. Interestingly, the Cu mass distribution at 24 h is very similar with that at 0.08 h, which may be related to the potential resistance mechanism of L. pneumophila cells.

To investigate the Cu contact time impact on L. pneumophila cell, the TC concentration and average Cu mass per cell were tested by SC-ICP-MS (Figures 8a and 8b). As shown in Figure 8a, the TC concentration decreased first then increased ($p > 0.05$) slightly over time. In the first 2 hours, TC concentration decreased rapidly and reached the highest disinfection rate of 62.9%. The Cu mass in individual L. pneumophila cell is shown in Figure 8b. Unlike the experiments exploring the impact of different Cu concentrations where the Cu mass per cell showed a linear increase with increasing Cu dosage, herein the Cu mass per cell showed a volatile upward pattern in the first 8 h.

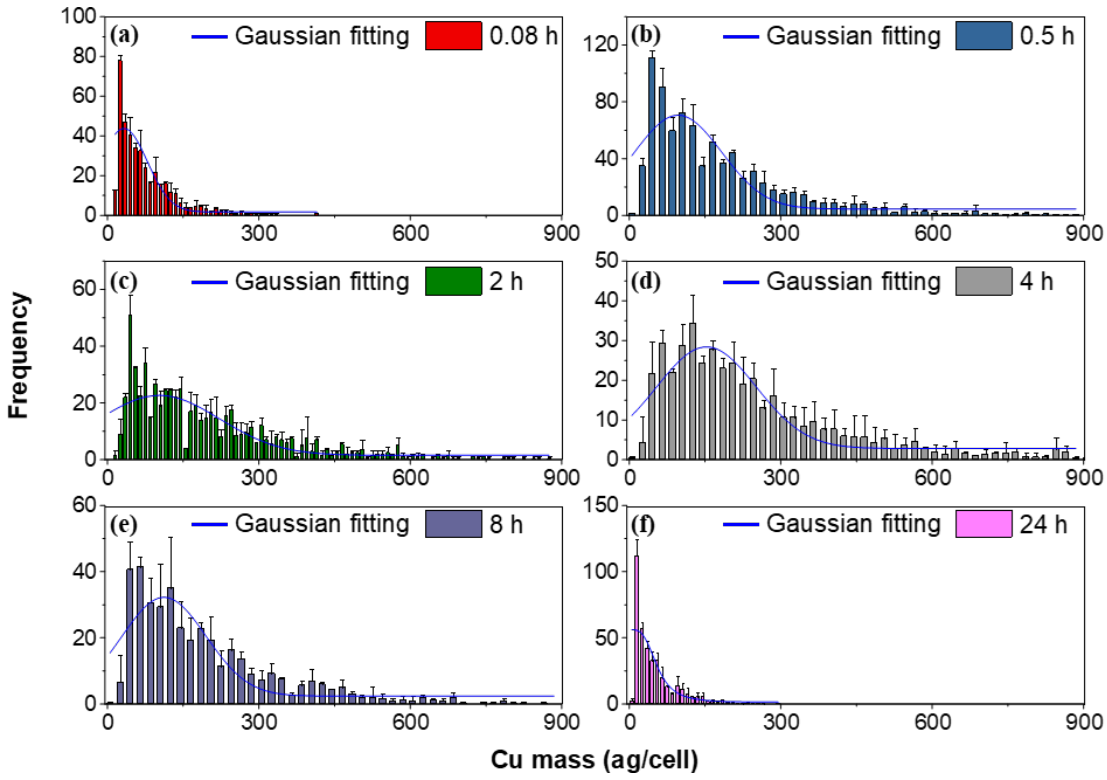

Figure 7. Histogram of Cu mass in individual L. pneumophila cell after treatments with different Cu contact times (a for 0.08 h; b for 0.5 h; c for 2 h; d for 4 h; e for 8 h; f for 24 h). The error bars in the SP-ICP-MS histograms represent standard deviation (n = 3).

For example, from 0.08 h to 0.5 h, the Cu mass increased by 133.3%, but it decreased by 8.6% from 0.5 h to 2 h. The similar phenomenon is also observed for the time period from 4 h to 8 h. Afterwards, a sharp decline (71.7%) was observed at 24 h and Cu mass in a single cell is close to 0.08 h. This particular variation pattern, fluctuating increase then decrease over time should be associated with the adjustment of L. pneumophila cells to adapt harsh environmental stressors and it may present the L. pneumophila cell's resistance to the Cu treatment quantitively.

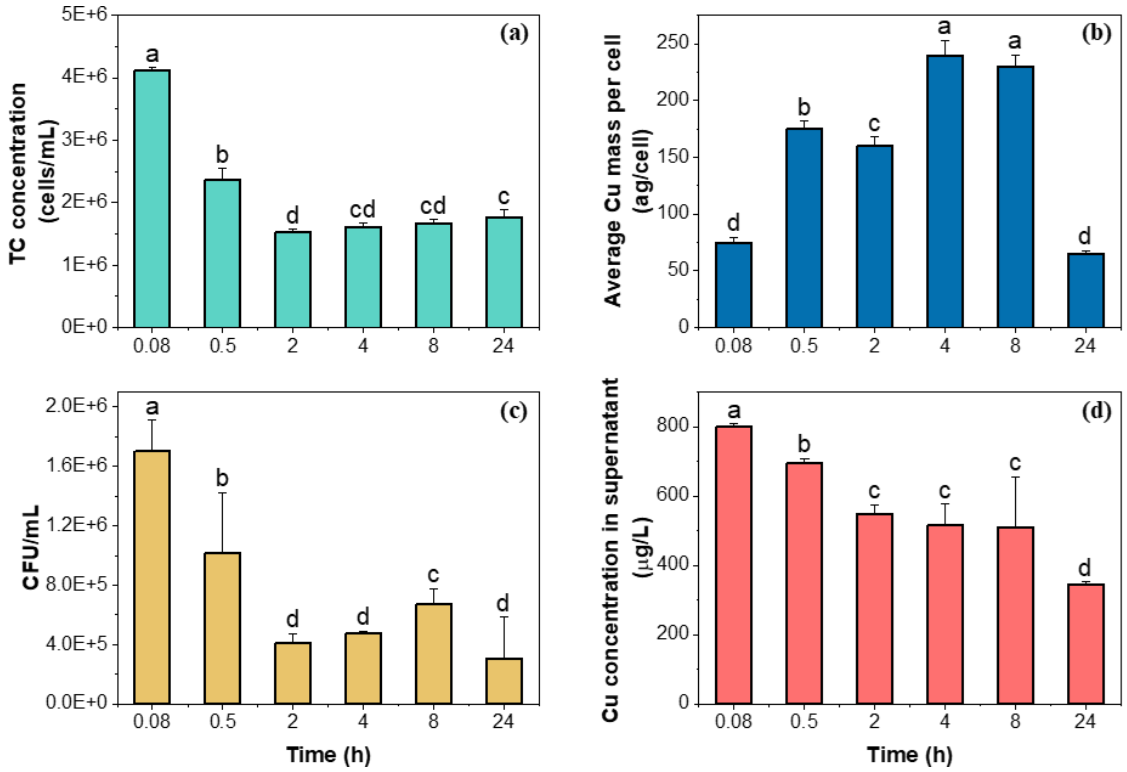

Figure 8. Cu contact time (0.08−24 h) effect on Legionella. (a) The variation of L. pneumophila cell concentration after the treatment with different Cu contact times; (b) Cu mass in individual L. pneumophila cell after the treatment with different Cu contact times; (c) CFU count of L. pneumophila cell after the treatment with different Cu contact times; (d) Cu concentration in supernatant after the treatment with different Cu contact times. Data are representative of three independent experiments and expressed as mean ± SD (n = 3, technical replicates). The statistical analysis was performed by IBM SPSS Statistics 27.0.1 using one-way ANOVA with Duncan's post-hoc test. Different letters indicate significant differences between different treatments ($p < 0.05$).

CFU counting experiment was further conducted to determine the change of VC cell concentration over time and subsequently evaluate the percentage profiles of VC, VBNC, and NVL cells. The percentage of NVBI cell was ignored due to the low level. The CFU counting displays a similar trend compared with the TC concentration detected by SC-ICP-MS, except at 24 h (Figure 8c). The highest VC disinfection rate was found at 24h. With the passage of Cu contact time, the ratio of NVL cell elevated first then decreased slightly, reaching highest level at 2 h. There is no obvious relationship between Cu contact time and VBNC cell ratio, further indicating that entering VBNC state of L. pneumophila cell is a decisive, regulated means to avoid Cu stress and prolong survival. The Cu concentrations in the supernatants were measured by the conventional ICP- MS method after the treatments of cell samples (Figure 8d). Cu concentration in the supernatant of Cu-treated water samples displayed an overall decreasing trend over time. Compared with dosed concentration of 800 μg/L, more than half of dosed Cu was lost from the supernatant after 24 h. SC-ICP-MS results also showed decreased cell concentrations due to cell death. As discussed in 3.2, the decreased Cu from the supernatant could result from the formation of Cu-related precipitation due to the existence of NOM, chloride, etc in real drinking water (9). In addition, because of the electrostatic adsorption effect between Cu ion and cell membrane, part of dosed Cu might adsorb to the cell surface and then be removed during centrifugation. The mechanism behind the relationship between Cu contact time and L. pneumophila cell concentration is likely multifactorial. Based on present study, it is not true that the longer the treatment time, the more efficient the disinfection. On the contrary, longer contact times can not only stimulate the bacteria's adaptive mechanism, the VBNC state, which increases the

risk of human infection, but lost more dissolved Cu due to the complicated drinking water matrix. Similar to our study, Song et al. found that Cu at a concentration of 800 μg/L inactivated L. pneumophila sharply after 4 h of exposure, but the antimicrobial effectiveness of Cu decreased after 6 h, with almost same log CFU reduction with 4 h (9). The rebound effect of L. pneumophila cell concentration over time is likely due to selective pressure, whereby the surviving bacterial populations exhibit increasing resistance to Cu toxicity. Research has proposed that bacterial resistance to Cu may arise due to prolonged exposure to sublethal concentrations of Cu, which facilitate the organism's survival with minimal inhibition. Inhibition, rather than complete elimination, exerts selective pressure that promotes the emergence of a more robust and resistant bacterial population (40). To a certain extent, L. pneumophila exhibits the capacity to neutralize Cu-generated ROS via the enzymatic action of superoxide dismutase. Superoxide dismutase catalyzes the conversion of superoxide radicals to hydrogen peroxide (H2O2), which is subsequently removed by the combined action of glutathione peroxidase-reductase and catalase, thereby effectively scavenging free radicals from the cellular environment (41, 42). In addition, June et al. reported that there are heavy metal efflux islands located on the L. pneumophila genome. One specific efflux system—Cu(I)-translocating P-type ATPase CopA, encoded by the gene lpg1024—is suggested to be responsible for L. pneumophila Cu resistance (35). The level of Cu mass in single cells in this study matches well with this report (Figure 8b). It showed that L. pneumophila cells uptake Cu rapidly in the first half hour, then slowed down the uptake, which may be due to the induction of this Cu efflux system. At 24 h, Cu mass per cell revised back to about the same as the 5 min contact time. This may be explained by the possibility that the cells

actively expelled the Cu ions, or most likely, a portion of cells never take up Cu. This portion of cells is likely to be the VBNC L. pneumophila as evidenced by these experimental results at 24 h contact time.

4. CONCLUSIONS

The present study developed a rapid and highly sensitive SC-ICP-MS method for investigation of L. pneumophila treatment by Cu. This SC-ICP-MS method can not only rapidly quantify the L. pneumophila cell concentration by monitoring 24Mg, but also accurately detect Cu concentration in the individual cells as well as Cu mass/cell distribution in the cell population to show the heterogeneity. The L. pneumophila cell concentration, average Cu mass per cell, CFU counts, and Cu concentration in supernatant all exhibited a dose-dependent tendency, with 800 and 1200 ug/L reaching similar high disinfection rates in drinking water. The investigation of percentages of VC, VBNC, NVBI, and NVL cells proved that Cu treatment can change VC cell to NVL cell effectively without forming NVBI cell, but Cu cannot affect the ratio of VBNC cell significantly. The contact time impact experiment demonstrated that there is no obvious proportional correlation between contact time and disinfection efficiency. The L. pneumophila cell possibly developed a bactericide resistant mechanism during treatment, or a portion of the L. pneumophila population, VBNC cells, never took up Cu during the treatment process. This novel methodology enables us to study the interaction of Cu and L. pneumophila quantitatively. This method is anticipated to be highly beneficial for understanding interactions between Legionella and metal disinfectants.

ACKNOWLEDGEMENTS

The United States Environmental Protection Agency (UA EPA) through its Office of Research and Development funded and collaborated in the research described here (SSWR.7.2.1). This article has been subjected to each US EPA's peer review and has been approved for publication. Mention of trade names or commercial products does not constitute endorsement or recommendation by the US EPA for use. The authors thank Dr. Paul K. Nam for his advice for the ICP-MS instrument and experiments. Authors are also appreciating Sargun Kaur for her help for the ICP-MS analysis method training. We also like to thank Gabrielle Hightower and Alex Daniels for the helping on Legionella cell culture.

STATEMENTS AND DECLARATIONS

***Funding**:* This study was funded by The United States Environmental Protection Agency (UA EPA) through its Office of Research and Development funded and collaborated in the research described here (SSWR.7.2.1).

***Conflict of interest**:* All the authors declare that they have no conflict of interest.

Availability of data and material: The data used in this study are available from the corresponding author upon reasonable request.

Code availability: Not applicable

Author Contribution Statement: All authors contributed to the study's conception and design. All authors commented on previous versions of the manuscript. AS developed the

SC-ICP-MS method and conducted SC-ICP-MS analyses, and edited the manuscript. XLconducted experiments with ICP-MS and SC-ICP-MS analyses and wrote the first draft of the manuscript, and edited the manuscript extensively. AC performed the cell culture, CFU count, and Cu treatment experiments and edited the manuscript. JL conceived and designed research and edited the manuscript. SE supervised the project and edited the manuscript. DW supervised the cell culture and edited the manuscript. HY supervised the project and edited the manuscript. HS conceived and designed research experiments and prepared the paper together with LX. All authors read and approved the final version of the manuscript.

Compliance with ethical standards*:* This article does not contain any studies with human and/or animal participants.

Ethics approval*:* Not applicable

Consent to participate: Not applicable

REFERENCES

1. Zhang C, Struewing I, Mistry JH, Wahman DG, Pressman J, Lu J. Legionella and other opportunistic pathogens in full-scale chloraminated municipal drinking water distribution systems. Water research. 2021;205:117571.

2. Beer KD, Gargano JW, Roberts VA, Hill VR, Garrison LE, Kutty PK, et al. Surveillance for waterborne disease outbreaks associated with drinking water—United States, 2011–2012. Morbidity and Mortality Weekly Report. 2015;64(31):842.

3. Benedict KM, Reses H, Vigar M, Roth DM, Roberts VA, Mattioli M, et al.Surveillance for waterborne disease outbreaks associated with drinking water—United States, 2013–2014. Morbidity and Mortality Weekly Report. 2017;66(44):1216.

4. Shah PP, Barskey AE, Binder AM, Edens C, Lee S, Smith JC, et al. Legionnaires' disease surveillance summary report, United States: 2014-1015. 2018.

5. Tsai K-P. Effects of two copper compounds on Microcystis aeruginosa cell density, membrane integrity, and microcystin release. Ecotoxicology and environmental safety. 2015;120:428-35.

6. Tsai K-P. Management of target algae by using copper-based algaecides: effects of algal cell density and sensitivity to copper. Water, Air, & Soil Pollution. 2016;227:1-11.

7. Hadjoudja S, Vignoles C, Deluchat V, Lenain J-F, Le Jeune A-H, Baudu M. Short term copper toxicity on Microcystis aeruginosa and Chlorella vulgaris using flow cytometry. Aquatic Toxicology. 2009;94(4):255-64.

8. Lin Y-sE, Vidic RD, Stout JE, Yu VL. Negative effect of high pH on biocidal efficacy of copper and silver ions in controlling Legionella pneumophila. Applied and environmental microbiology. 2002;68(6):2711-5.

9. Song Y, Pruden A, Edwards MA, Rhoads WJ. Natural organic matter, orthophosphate, pH, and growth phase can limit copper antimicrobial efficacy for Legionella in drinking water. Environmental Science & Technology. 2021;55(3):1759-68.

10. Vincent M, Hartemann P, Engels-Deutsch M. Antimicrobial applications of copper. International journal of hygiene and environmental health. 2016;219(7):585-91.

11. Cloutman-Green E, Barbosa VL, Jimenez D, Wong D, Dunn H, Needham B, et al. Controlling Legionella pneumophila in water systems at reduced hot water temperatures with copper and silver ionization. American Journal of Infection Control. 2019;47(7):761- 6.

12. Bédard E, Trigui H, Liang J, Doberva M, Paranjape K, Lalancette C, et al. Local adaptation of Legionella pneumophila within a hospital hot water system increases tolerance to copper. Applied and Environmental Microbiology. 2021;87(10):e00242-21.

13. Zheng L-N, Wang M, Wang B, Chen H-Q, Ouyang H, Zhao Y-L, et al. Determination of quantum dots in single cells by inductively coupled plasma mass spectrometry. Talanta. 2013;116:782-7.

14. Mueller L, Traub H, Jakubowski N, Drescher D, Baranov VI, Kneipp J. Trends in single-cell analysis by use of ICP-MS. Analytical and Bioanalytical Chemistry. 2014;406(27):6963-77.

15. Mueller L, Traub H, Jakubowski N, Drescher D, Baranov VI, Kneipp J. Trends in single-cell analysis by use of ICP-MS. Analytical and bioanalytical chemistry. 2014;406:6963-77.

16. Rasmussen L, Shi H, Liu W, Shannon KB. Quantification of silver nanoparticle interactions with yeast Saccharomyces cerevisiae studied using single-cell ICP-MS. Analytical and Bioanalytical Chemistry. 2022;414(9):3077-86.

17. Groombridge AS, Miyashita S-i, Fujii S-i, Nagasawa K, Okahashi T, Ohata M, et al. High sensitive elemental analysis of single yeast cells (Saccharomyces cerevisiae) by time-resolved inductively-coupled plasma mass spectrometry using a high efficiency cell introduction system. Analytical Sciences. 2013;29(6):597-603.

18. Wang H, Wang B, Wang M, Zheng L, Chen H, Chai Z, et al. Time-resolved ICP-MS analysis of mineral element contents and distribution patterns in single cells. Analyst. 2015;140(2):523-31.

19. Shen X, Zhang H, He X, Shi H, Stephan C, Jiang H, et al. Evaluating the treatment effectiveness of copper-based algaecides on toxic algae Microcystis aeruginosa using single cell-inductively coupled plasma-mass spectrometry. Analytical and bioanalytical chemistry. 2019;411:5531-43.

20. Tsang C-N, Ho K-S, Sun H, Chan W-T. Tracking bismuth antiulcer drug uptake in single Helicobacter pylori cells. Journal of the American Chemical Society. 2011;133(19):7355-7.

21. Wang H, Wang M, Wang B, Zheng L, Chen H, Chai Z, et al. Interrogating the variation of element masses and distribution patterns in single cells using ICP-MS with a high efficiency cell introduction system. Analytical and bioanalytical chemistry. 2017;409:1415-23.

22. Merrifield R, Stephan C, Lead J. Quantification of Au nanoparticle biouptake and distribution to freshwater algae using single cell–ICP-MS. Environmental science & technology. 2018;52(4):2271-7.

23. Meyer S, López-Serrano A, Mitze H, Jakubowski N, Schwerdtle T. Single-cell analysis by ICP-MS/MS as a fast tool for cellular bioavailability studies of arsenite. Metallomics. 2018;10(1):73-6.

24. Virani F, Tanner S. Mass cytometry: an evolution in ICP-MS enabling novel insights in single-cell biology. Spectroscopy. 2015;30(5).

25. Oliver AL-S, Baumgart S, Bremser W, Flemig S, Wittke D, Grützkau A, et al. Quantification of silver nanoparticles taken up by single cells using inductively coupled plasma mass spectrometry in the single cell measurement mode. Journal of Analytical Atomic Spectrometry. 2018;33(7):1256-63.

26. Lim SY, Low ZE, Tan RPW, Lim ZC, Ang WH, Kubota T, et al. Single-cell and bulk ICP–MS investigation of accumulation patterns of Pt-based metallodrugs in cisplatin- sensitive and-resistant cell models. Metallomics. 2022;14(12):mfac085.

27. da Silva ABS, Arruda MAZ. Single-cell ICP-MS to address the role of trace elements at a cellular level. Journal of Trace Elements in Medicine and Biology. 2022:127086.

28. Buse HY, Brehm A, Santo Domingo JW, Ashbolt NJ. Screening-level assays for potentially human-infectious environmental Legionella spp. The Journal of Microbiology. 2011;49(2):200-7.

29. Jepras R, Clarke D, Coakley W. Agglutination of Legionella pneumophila by antiserum is accelerated in an ultrasonic standing wave. Journal of immunological methods. 1989;120(2):201-5.

30. Sandle T. Ready for the count? Back-to-basics review of microbial colony counting. Journal of GxP Compliance. 2020;24(1).

31. Hans M, Támara JC, Mathews S, Bax B, Hegetschweiler A, Kautenburger R, et al. Laser cladding of stainless steel with a copper–silver alloy to generate surfaces of high antimicrobial activity. Applied Surface Science. 2014;320:195-9.

32. Grass G, Rensing C, Solioz M. Metallic copper as an antimicrobial surface. Applied and environmental microbiology. 2011;77(5):1541-7.

33. Godoy-Gallardo M, Eckhard U, Delgado LM, de Roo Puente YJ, Hoyos-Nogués M, Gil FJ, et al. Antibacterial approaches in tissue engineering using metal ions and nanoparticles: From mechanisms to applications. Bioactive Materials. 2021;6(12):4470- 90.

34. Stohs SJ, Bagchi D. Oxidative mechanisms in the toxicity of metal ions. Free radical biology and medicine. 1995;18(2):321-36.

35. June SG, Dziewulski DM. Copper and silver biocidal mechanisms, resistance strategies, and efficacy for legionella control. Journal-American Water Works Association. 2018;110(12):E13-E35.

36. Cai Y, Liu J, Li G, Wong PK, An T. Formation mechanisms of viable but nonculturable bacteria through induction by light-based disinfection and their antibiotic resistance gene transfer risk: A review. Critical Reviews in Environmental Science and Technology. 2022;52(20):3651-88.

37. Bodor A, Bounedjoum N, Vincze GE, Erdeiné Kis Á, Laczi K, Bende G, et al. Challenges of unculturable bacteria: environmental perspectives. Reviews in Environmental Science and Bio/Technology. 2020;19:1-22.

38. Dong K, Pan H, Yang D, Rao L, Zhao L, Wang Y, et al. Induction, detection, formation, and resuscitation of viable but non-culturable state microorganisms. Comprehensive Reviews in Food Science and Food Safety. 2020;19(1):149-83.

39. Robertson P, Abdelhady H, Garduño RA. The many forms of a pleomorphic bacterial pathogen—the developmental network of Legionella pneumophila. Frontiers in microbiology. 2014;5:670.

40. Warnes S, Green S, Michels H, Keevil C. Biocidal efficacy of copper alloys against pathogenic enterococci involves degradation of genomic and plasmid DNAs. Applied and environmental microbiology. 2010;76(16):5390-401.

41. Lemire JA, Harrison JJ, Turner RJ. Antimicrobial activity of metals: mechanisms, molecular targets and applications. Nature Reviews Microbiology. 2013;11(6):371-84.

42. Cross J, Currier R, Torraco D, Vanderberg L, Wagner G, Gladen P. Killing of Bacillus spores by aqueous dissolved oxygen, ascorbic acid, and copper ions. Applied and environmental microbiology. 2003;69(4):2245-52.

SECTION

2. CONCLUSIONS

Pathological processes of public health concern are a significant and growing area of bioanalytical chemistry research. In our work, we have attempted to address two public health concerns, traumatic brain injury (TBI) and L. pneumophilia contamination of domestic water systems. On the TBI front, we have developed two HPLC-MS/MS methods and applied those to a cohort of soldiers undergoing blast related training. In the longitudinal study, we found significant differences in several analytes in our proposed biomarker panel which are worthy of further pursuit. As for L. pneumophilia contamination, we have established single cell ICP-MS methodologies to study disinfection by Cu. The investigation of percentages of VC, VBNC, NVBI, and NVL cells proved that Cu treatment can change VC cell to NVL cell effectively without forming NVBI cell, but Cu cannot affect the ratio of VBNC cell significantly. The contact time impact experiment additionally demonstrated that there is no obvious proportional correlation between contact time and disinfection efficiency. Finally, this ICP-MS method is also feasible to study disinfection by other disinfectants, especially to study the cell viable culturable and non-culturable nature of legionella. We hope that this work will spark additional research to improve the lives of individuals and communities which suffer from these and other pathologies.

BIBLIOGRAPHY

[1] Y. Y. Broza et al., "Disease Detection with Molecular Biomarkers: From Chemistry of Body Fluids to Nature-Inspired Chemical Sensors," Chemical Reviews, vol. 119, no. 22. American Chemical Society, pp. 11761–11817, Nov. 27,2019. doi: 10.1021/acs.chemrev.9b00437.

[2] C. A. Crutchfield, S. N. Thomas, L. J. Sokoll, and D. W. Chan, "Advances in mass spectrometry-based clinical biomarker discovery," Clinical Proteomics, vol. 13, no. 1. BioMed Central Ltd., Jan. 07, 2016. doi: 10.1186/s12014-015-9102-9.

[3] C. Fernández-Metzler et al., "Biomarker Assay Validation by Mass Spectrometry," AAPS Journal, vol. 24, no. 3, May 2022, doi: 10.1208/s12248-022- 00707-z.

[4] F. Cai et al., "Screening of lipid metabolism biomarkers in patients with coronary heart disease via ultra-performance liquid chromatography–high resolution mass spectrometry," Journal of Chromatography B, vol. 1169, p. 122603, Apr. 2021, doi: 10.1016/j.jchromb.2021.122603.

[5] Y. Mechref, Y. Hu, A. Garcia, and A. Hussein, "Identifying cancer biomarkers by mass spectrometry-based glycomics," Electrophoresis, vol. 33, no. 12, pp. 1755–1767, Jul. 2012, doi: 10.1002/elps.201100715.

[6] X. Zhang, D. Wei, Y. Yap, L. Li, S. Guo, and F. Chen, "Mass spectrometry-based 'omics' technologies in cancer diagnostics," Mass Spectrom Rev, vol. 26, no. 3, pp. 403–431, May 2007, doi: 10.1002/mas.20132.

[7] A. Macklin, S. Khan, and T. Kislinger, "Recent advances in mass spectrometry based clinical proteomics: Applications to cancer research," Clinical Proteomics, vol. 17, no. 1. BioMed Central Ltd., May 24, 2020. doi: 10.1186/s12014-020-09283-w.

[8] M. W. Bourassa and L. M. Miller, "Metal imaging in neurodegenerative diseases," Metallomics, vol. 4, no. 8. pp. 721–738, Aug. 2012. doi: 10.1039/c2mt20052j.

[9] W. Michno, P. M. Wehrli, K. Blennow, H. Zetterberg, and J. Hanrieder, "Molecular imaging mass spectrometry for probing protein dynamics in neurodegenerative disease pathology," Journal of Neurochemistry, vol. 151, no. 4. Blackwell Publishing Ltd, pp. 488–506, Nov. 01, 2019. doi: 10.1111/jnc.14559.

[10] E. J. Want, B. F. Cravatt, and G. Siuzdak, "The expanding role of mass spectrometry in metabolite profiling and characterization," ChemBioChem, vol. 6, no. 11. pp. 1941–1951, Nov. 2005. doi: 10.1002/cbic.200500151.

[11] D. of Health, H. Services, and C. for Disease Control, “Centers for Disease Control and Prevention Prevention and Control SURVEILLANCE REPORT Surveillance Report of Traumatic Brain Injury-related Emergency Department Visits, Hospitalizations, and Deaths TBI: SURVEILLANCE REPORT ACKNOWLEDGEMENTS.” [Online]. Available: www.cdc.gov/TraumaticBrainInjury

[12] A. K. Shetty, V. Mishra, M. Kodali, and B. Hattiangady, “Blood brain barrier dysfunction and delayed neurological deficits in mild traumatic brain injury induced by blast shock waves,” Front Cell Neurosci, vol. 8, Aug. 2014, doi: 10.3389/fncel.2014.00232.

[13] K. S. Tanev, K. Z. Pentel, M. A. Kredlow, and M. E. Charney, “PTSD and TBI co-morbidity: Scope, clinical presentation and treatment options,” Brain Inj, vol. 28, no. 3, pp. 261–270, Mar. 2014, doi: 10.3109/02699052.2013.873821.

[14] T. M. Sivanandam and M. K. Thakur, “Traumatic brain injury: A risk factor for Alzheimer’s disease,” Neurosci Biobehav Rev, vol. 36, no. 5, pp. 1376–1381, May 2012, doi: 10.1016/J.NEUBIOREV.2012.02.013.

[15] K. A. Jellinger, “Blunt Traumatic Brain Injury and Alzheimer Pathology,” Dement Geriatr Cogn Disord, Jan. 2022, doi: 10.1159/000527686.

[16] M. P. Murphy and H. Carmine, “Long-term health implications of individuals with TBI: A rehabilitation perspective,” NeuroRehabilitation, vol. 31, no. 1, pp. 85–94, Apr. 2012, doi: 10.3233/NRE-2012-0777.

[17] K. S. Gilbert, S. M. Kark, P. Gehrman, and Y. Bogdanova, “Sleep disturbances, TBI and PTSD: Implications for treatment and recovery,” Clin Psychol Rev, vol. 40, pp. 195–212, Aug. 2015, doi: 10.1016/J.CPR.2015.05.008.

[18] A. I. R. Maas et al., “Traumatic brain injury: integrated approaches to improve prevention, clinical care, and research,” Lancet Neurol, vol. 16, no. 12, pp. 987–1048, Dec. 2017, doi: 10.1016/S1474-4422(17)30371-X.

[19] J. R. Kulbe and J. W. Geddes, “Current status of fluid biomarkers in mild traumatic brain injury,” Exp Neurol, vol. 275, pp. 334–352, Jan. 2016, doi: 10.1016/j.expneurol.2015.05.004.

[20] E. Czeiter et al., “Blood biomarkers on admission in acute traumatic brain injury: Relations to severity, CT findings and care path in the CENTER-TBI study,” EBioMedicine, vol. 56, p. 102785, Jun. 2020, doi: 10.1016/j.ebiom.2020.102785.

[21] K. K. Wang et al., “An update on diagnostic and prognostic biomarkers for traumatic brain injury,” Expert Rev Mol Diagn, vol. 18, no. 2, pp. 165–180, Feb. 2018, doi: 10.1080/14737159.2018.1428089.

[22] Z. S. Gan et al., “Blood Biomarkers for Traumatic Brain Injury: A Quantitative Assessment of Diagnostic and Prognostic Accuracy,” Front Neurol, vol. 10, Apr. 2019, doi: 10.3389/fneur.2019.00446.

[23] L. Papa et al., “Serum levels of ubiquitin C-terminal hydrolase distinguish mild traumatic brain injury from trauma controls and are elevated in mild and moderate traumatic brain injury patients with intracranial lesions and neurosurgical intervention,” Journal of Trauma and Acute Care Surgery, vol. 72, no. 5, pp. 1335–1344, May 2012, doi: 10.1097/TA.0b013e3182491e3d.

[24] S. Shahjouei et al., “The diagnostic values of UCH-L1 in traumatic brain injury: A meta-analysis,” Brain Inj, vol. 32, no. 1, pp. 1–17, Jan. 2018, doi: 10.1080/02699052.2017.1382717.

[25] J. J. Bazarian et al., “Serum GFAP and UCH-L1 for prediction of absence of intracranial injuries on head CT (ALERT-TBI): a multicentre observational study,” Lancet Neurol, vol. 17, no. 9, pp. 782–789, Sep. 2018, doi: 10.1016/S1474-4422(18)30231-X.

[26] K. Nylén et al., “Increased serum-GFAP in patients with severe traumatic brain injury is related to outcome,” J Neurol Sci, vol. 240, no. 1–2, pp. 85–91, Jan. 2006, doi: 10.1016/J.JNS.2005.09.007.

[27] E. P. Thelin, D. W. Nelson, and B. M. Bellander, “A review of the clinical utility of serum S100B protein levels in the assessment of traumatic brain injury,” Acta Neurochirurgica, vol. 159, no. 2. Springer-Verlag Wien, pp. 209–225, Feb. 01, 2017. doi: 10.1007/s00701-016-3046-3.

[28] M. P. MacFarlane and T. C. Glenn, “Neurochemical cascade of concussion,” Brain Inj, vol. 29, no. 2, pp. 139–153, Jan. 2015, doi: 10.3109/02699052.2014.965208.

[29] R. M. Guerriero, C. C. Giza, and A. Rotenberg, “Glutamate and GABA Imbalance Following Traumatic Brain Injury,” Curr Neurol Neurosci Rep, vol. 15, no. 5, p. 27, May 2015, doi: 10.1007/s11910-015-0545-1.

[30] A. J. Baker, R. J. Moulton, V. H. MacMillan, and P. M. Shedden, “Excitatory amino acids in cerebrospinal fluid following traumatic brain injury in humans,” J Neurosurg, vol. 79, no. 3, pp. 369–372, Sep. 1993, doi: 10.3171/jns.1993.79.3.0369.

[31] J. E. Ozga, J. M. Povroznik, E. B. Engler-Chiurazzi, and C. V. Haar, “Executive (dys)function after traumatic brain injury: special considerations for behavioral pharmacology,” Behavioural Pharmacology, vol. 29, no. 7, pp. 617–637, Oct. 2018, doi: 10.1097/FBP.0000000000000430.

[32] A. K. Wagner, A. E. Kline, J. Sokoloski, R. D. Zafonte, E. Capulong, and C. E. Dixon, “Intervention with environmental enrichment after experimental brain trauma enhances cognitive recovery in male but not female rats,” Neurosci Lett, vol. 334, no. 3, pp. 165–168, Dec. 2002, doi: 10.1016/S0304-3940(02)01103-5.

[33] N. Khatri, M. Thakur, V. Pareek, S. Kumar, S. Sharma, and A. K. Datusalia, “Oxidative Stress: Major Threat in Traumatic Brain Injury,” CNS Neurol Disord Drug Targets, vol. 17, no. 9, pp. 689–695, Nov. 2018, doi: 10.2174/1871527317666180627120501.

[34] E. M. Lutton et al., “Endothelial Targeted Strategies to Combat Oxidative Stress: Improving Outcomes in Traumatic Brain Injury,” Front Neurol, vol. 10, Jun. 2019, doi: 10.3389/fneur.2019.00582.

[35] R. J. Shannon et al., “Extracellular N -Acetylaspartate in Human Traumatic Brain Injury,” J Neurotrauma, vol. 33, no. 4, pp. 319–329, Feb. 2016, doi: 10.1089/neu.2015.3950.

[36] F. Clausen, N. Marklund, A. Lewén, P. Enblad, S. Basu, and L. Hillered, “Interstitial F 2 -Isoprostane 8-Iso-PGF 2α As a Biomarker of Oxidative Stress after Severe Human Traumatic Brain Injury,” J Neurotrauma, vol. 29, no. 5, pp. 766–775, Mar. 2012, doi: 10.1089/neu.2011.1754.

[37] J. qing Lai, Y. C. Shi, S. Lin, and X. R. Chen, “Metabolic disorders on cognitive dysfunction after traumatic brain injury,” Trends in Endocrinology and Metabolism, vol. 33, no. 7. Elsevier Inc., pp. 451–462, Jul. 01, 2022. doi: 10.1016/j.tem.2022.04.003.

[38] A. M. Lamade, T. S. Anthonymuthu, Z. E. Hier, Y. Gao, V. E. Kagan, and H. Bayır, “Mitochondrial damage & lipid signaling in traumatic brain injury,” Exp Neurol, vol. 329, p. 113307, Jul. 2020, doi: 10.1016/J.EXPNEUROL.2020.113307.

[39] T. S. Anthonymuthu et al., “Global assessment of oxidized free fatty acids in brain reveals an enzymatic predominance to oxidative signaling after trauma,” Biochimica et Biophysica Acta (BBA) - Molecular Basis of Disease, vol. 1863, no. 10, pp. 2601–2613, Oct. 2017, doi: 10.1016/J.BBADIS.2017.03.015.

[40] S. Zhang, B. B. Lachance, M. P. Mattson, and X. Jia, “Glucose metabolic crosstalk and regulation in brain function and diseases,” Prog Neurobiol, vol. 204, p. 102089, Sep. 2021, doi: 10.1016/J.PNEUROBIO.2021.102089.

[41] K. L. H. Carpenter, I. Jalloh, and P. J. Hutchinson, “Glycolysis and the significance of lactate in traumatic brain injury,” Frontiers in Neuroscience, vol. 9, no. APR. Frontiers Research Foundation, 2015. doi: 10.3389/fnins.2015.00112.

[42] H. Zetterberg, D. H. Smith, and K. Blennow, “Biomarkers of mild traumatic brain injury in cerebrospinal fluid and blood,” Nat Rev Neurol, vol. 9, no. 4, pp. 201–210, Apr. 2013, doi: 10.1038/nrneurol.2013.9.

[43] J. L. Luque-Garcia and T. A. Neubert, “Sample preparation for serum/plasma profiling and biomarker identification by mass spectrometry,” J Chromatogr A, vol. 1153, no. 1–2, pp. 259–276, Jun. 2007, doi: 10.1016/J.CHROMA.2006.11.054.

[44] S. Bouatra et al., “The Human Urine Metabolome,” PLoS One, vol. 8, no. 9, Sep.2013, doi: 10.1371/journal.pone.0073076.

[45] J. Rodríguez-Morató, Ó. J. Pozo, and J. Marcos, “Targeting human urinary metabolome by LC–MS/MS: a review,” Bioanalysis, vol. 10, no. 7, pp. 489–516, Apr. 2018, doi: 10.4155/bio-2017-0285.

[46] J. R. Kulbe and J. W. Geddes, “Current status of fluid biomarkers in mild traumatic brain injury,” Exp Neurol, vol. 275, pp. 334–352, Jan. 2016, doi: 10.1016/J.EXPNEUROL.2015.05.004.

[47] N. le Sage et al., “Detection of S-100β protein in plasma and urine after a mild traumatic brain injury,” Canadian Journal of Neurological Sciences, vol. 46, no. 5, pp. 599–602, Sep. 2019, doi: 10.1017/cjn.2019.61.

[48] A. Rodríguez-Rodríguez et al., “Role of S100B protein in urine and serum as an early predictor of mortality after severe traumatic brain injury in adults,” Clinica Chimica Acta, vol. 414, pp. 228–233, Dec. 2012, doi: 10.1016/J.CCA.2012.09.025.

[49] S. Mondello et al., “The Challenge of Mild Traumatic Brain Injury: Role of Biochemical Markers in Diagnosis of Brain Damage,” Med Res Rev, vol. 34, no. 3, pp. 503–531, May 2014, doi: 10.1002/med.21295.

[50] J. E. Bailes, A. L. Petraglia, B. I. Omalu, E. Nauman, and T. Talavage, “Role of subconcussion in repetitive mild traumatic brain injury,” J Neurosurg, vol. 119, no. 5, pp. 1235–1245, Nov. 2013, doi: 10.3171/2013.7.JNS121822.

[51] S. M. Slobounov et al., “The effect of repetitive subconcussive collisions on brain integrity in collegiate football players over a single football season: A multi-modal neuroimaging study,” Neuroimage Clin, vol. 14, pp. 708–718, 2017, doi: 10.1016/j.nicl.2017.03.006.

[52] X. Xu et al., “Repetitive mild traumatic brain injury in mice triggers a slowly developing cascade of long-term and persistent behavioral deficits and pathological changes,” Acta Neuropathol Commun, vol. 9, no. 1, p. 60, Dec. 2021, doi: 10.1186/s40478-021-01161-2.

[53] W. Carr et al., “Repeated Low-Level Blast Exposure: A Descriptive Human Subjects Study,” Mil Med, vol. 181, no. 5S, pp. 28–39, May 2016, doi: 10.7205/MILMED-D-15-00137.

[54] M. Lindberg, S. Sloley, B. Ivins, D. Marion, and E. Moy Martin, “Military TBI—What civilian primary care providers should know,” J Family Med Prim Care, vol. 10, no. 12, p. 4391, 2021, doi: 10.4103/jfmpc.jfmpc_98_21.

[55] W. Carr et al., “Relation of Repeated Low-Level Blast Exposure With Symptomology Similar to Concussion,” Journal of Head Trauma Rehabilitation, vol. 30, no. 1, pp. 47–55, Jan. 2015, doi: 10.1097/HTR.0000000000000064.

[56] D. L. Dickstein et al., “Brain and blood biomarkers of tauopathy and neuronal injury in humans and rats with neurobehavioral syndromes following blast exposure,” Mol Psychiatry, vol. 26, no. 10, pp. 5940–5954, Oct. 2021, doi: 10.1038/s41380-020-0674-z.

[57] B. A. Schultz, D. X. Cifu, S. McNamee, M. Nichols, and W. Carne, “Assessment and treatment of common persistent sequelae following blast induced mild traumatic brain injury,” NeuroRehabilitation, vol. 28, no. 4, pp. 309–320, Jun. 2011, doi: 10.3233/NRE-2011-0659.

[58] H. Song et al., “Ultrastructural brain abnormalities and associated behavioral changes in mice after low-intensity blast exposure,” Behavioural Brain Research, vol. 347, pp. 148–157, Jul. 2018, doi: 10.1016/j.bbr.2018.03.007.

[59] N. D. Osier and C. E. Dixon, “The controlled cortical impact model: Applications, considerations for researchers, and future directions,” Frontiers in Neurology, vol. 7, no. AUG. Frontiers Media S.A., Aug. 02, 2016. doi: 10.3389/fneur.2016.00134.

[60] J. Lifshitz, “Fluid Percussion Injury Model,” 2009, pp. 369–384. doi: 10.1007/978-1-60327-185-1_32.

[61] H. Song et al., “Linking blast physics to biological outcomes in mild traumatic brain injury: Narrative review and preliminary report of an open-field blast model,” Behavioural Brain Research, vol. 340, pp. 147–158, Mar. 2018, doi: 10.1016/j.bbr.2016.08.037.

[62] A. Khodr et al., “Molecular epidemiology, phylogeny and evolution of Legionella,” Infection, Genetics and Evolution, vol. 43, pp. 108–122, Sep. 2016, doi: 10.1016/J.MEEGID.2016.04.033.

[63] N. Phin et al., “Epidemiology and clinical management of Legionnaires’ disease,” Lancet Infect Dis, vol. 14, no. 10, pp. 1011–1021, Oct. 2014, doi: 10.1016/S1473-3099(14)70713-3.

[64] E. Leoni, G. De Luca, P. P. Legnani, R. Sacchetti, S. Stampi, and F. Zanetti, “Legionella waterline colonization: detection of Legionella species in domestic, hotel and hospital hot water systems,” J Appl Microbiol, vol. 98, no. 2, pp. 373–379, Feb. 2005, doi: 10.1111/j.1365-2672.2004.02458.x.

[65] J. P. Springston and L. Yocavitch, “Existence and control of Legionella bacteria in building water systems: A review,” J Occup Environ Hyg, vol. 14, no. 2, pp. 124–134, Feb. 2017, doi: 10.1080/15459624.2016.1229481.

[66] S. M. Walser, D. G. Gerstner, B. Brenner, C. Höller, B. Liebl, and C. E. W. Herr, “Assessing the environmental health relevance of cooling towers – A systematic review of legionellosis outbreaks,” Int J Hyg Environ Health, vol. 217, no. 2–3,pp. 145–154, Mar. 2014, doi: 10.1016/j.ijheh.2013.08.002.

[67] A. J. Prussin, D. O. Schwake, and L. C. Marr, “Ten questions concerning the aerosolization and transmission of Legionella in the built environment,” Build Environ, vol. 123, pp. 684–695, Oct. 2017, doi: 10.1016/J.BUILDENV.2017.06.024.

[68] E. Van Heijnsbergen, J. A. C. Schalk, S. M. Euser, P. S. Brandsema, J. W. Den Boer, and A. M. De Roda Husman, “Confirmed and potential sources of Legionella reviewed,” Environ Sci Technol, vol. 49, no. 8, pp. 4797–4815, Apr. 2015, doi: 10.1021/ACS.EST.5B00142.

[69] T. Lupia et al., “Legionella pneumophila Infections during a 7-Year Retrospective Analysis (2016–2022): Epidemiological, Clinical Features and Outcomes in Patients with Legionnaires’ Disease,” Microorganisms, vol. 11, no. 2, Feb. 2023, doi: 10.3390/MICROORGANISMS11020498.

[70] A. H. Havelaar et al., “Balancing the Risks and Benefits of Drinking Water Disinfection: Disability Adjusted Life-Years on the Scale,” 2000.

[71] M. A. Mazhar et al., “Chlorination disinfection by-products in municipal drinking water – A review,” Journal of Cleaner Production, vol. 273. Elsevier Ltd, Nov. 10, 2020. doi: 10.1016/j.jclepro.2020.123159.

[72] A. Srinivasan et al., “A 17-Month Evaluation of a Chlorine Dioxide Water Treatment System to Control Legionella Species in a Hospital Water Supply,” Infect Control Hosp Epidemiol, vol. 24, no. 8, pp. 575–579, Aug. 2003, doi: 10.1086/502254.

[73] A. Bruchet, E. Costentin, M. F. Legrand, and J. Mallevialle, “Influence of the Chlorination of Natural Nitrogenous Organic Compounds on Tastes and Odors in Finished Drinking Waters,” Water Science and Technology, vol. 25, no. 2, pp. 323–333, Jan. 1992, doi: 10.2166/wst.1992.0068.

[74] R. H. Burttschell, A. A. Rosen, and F. M. Middleton, “Chlorine Derivatives of Phenol Causing Taste and Odor,” 1959.

[75] I. Y. Roi, N. A. Klimenko, G. M. Zdorovenko, and V. V. Goncharuk, “Species identification of water microorganisms resistant to chlorine compounds,” Journal of Water Chemistry and Technology, vol. 37, no. 3, pp. 145–150, May 2015, doi: 10.3103/S1063455X1503008X.

[76] L. W. Luo et al., “Evaluating method and potential risks of chlorine-resistant bacteria (CRB): A review,” Water Res, vol. 188, p. 116474, Jan. 2021, doi: 10.1016/J.WATRES.2020.116474.

[77] J. M. Kuchta et al., “Enhanced Chlorine Resistance of Tap Water-Adapted Legionella pneumophila as Compared with Agar Medium-Passaged Strains,” 1985. [Online]. Available: https://journals.asm.org/journal/aem

[78] S. W. Krasner et al., “Occurrence of a new generation of disinfection byproducts,” Environ Sci Technol, vol. 40, no. 23, pp. 7175–7185, Dec. 2006, doi: 10.1021/es060353j.

[79] X. F. Li and W. A. Mitch, “Drinking Water Disinfection Byproducts (DBPs) and Human Health Effects: Multidisciplinary Challenges and Opportunities,” Environ Sci Technol, vol. 52, no. 4, pp. 1681–1689, Feb. 2018, doi: 10.1021/acs.est.7b05440.

[80] R. Dewil, D. Mantzavinos, I. Poulios, and M. A. Rodrigo, “New perspectives for Advanced Oxidation Processes,” J Environ Manage, vol. 195, pp. 93–99, Jun. 2017, doi: 10.1016/J.JENVMAN.2017.04.010.

[81] I. Sirés, E. Brillas, M. A. Oturan, M. A. Rodrigo, and M. Panizza, “Electrochemical advanced oxidation processes: Today and tomorrow. A review,” Environmental Science and Pollution Research, vol. 21, no. 14, pp. 8336–8367, 2014, doi: 10.1007/s11356-014-2783-1.

[82] R. B. P. Marcelino, M. M. D. Leão, R. M. Lago, and C. C. Amorim, “Multistage ozone and biological treatment system for real wastewater containing antibiotics,” J Environ Manage, vol. 195, pp. 110–116, Jun. 2017, doi: 10.1016/j.jenvman.2016.04.041.

[83] J. G. Jacangelo, N. L. Patania, K. M. Reagan, E. M. Aieta, S. W. Krasner, and M.J. McGuire, “Ozonation: Assessing Its Role in the Formation and Control of Disinfection By-products,” J Am Water Works Assoc, vol. 81, no. 8, pp. 74–84, Aug. 1989, doi: 10.1002/j.1551-8833.1989.tb03262.x.

[84] A. D. Shah and W. A. Mitch, “Halonitroalkanes, halonitriles, haloamides, and N-nitrosamines: A critical review of nitrogenous disinfection byproduct formation pathways,” Environmental Science and Technology, vol. 46, no. 1. pp. 119–131, Jan. 03, 2012. doi: 10.1021/es203312s.

[85] Q. Gao and A. A. Keller, “Redesigning Water Disinfection Using Recyclable Nanomaterials and Metal Ions: Evaluation with Escherichia coli,” ACS Environmental Science and Technology Water, vol. 1, no. 1, pp. 185–194, Jan. 2021, doi: 10.1021/acsestwater.0c00066.

[86] A. Sirelkhatim et al., “Review on zinc oxide nanoparticles: Antibacterial activity and toxicity mechanism,” Nanomicro Lett, vol. 7, no. 3, pp. 219–242, Apr. 2015, doi: 10.1007/S40820-015-0040-X.

[87] E. A. S. Dimapilis, C. S. Hsu, R. M. O. Mendoza, and M. C. Lu, “Zinc oxide nanoparticles for water disinfection,” Sustainable Environment Research, vol. 28, no. 2, pp. 47–56, Mar. 2018, doi: 10.1016/J.SERJ.2017.10.001.

[88] R. Castro-Muñoz, “The Role of New Inorganic Materials in Composite Membranes for Water Disinfection,” Membranes (Basel), vol. 10, no. 5, p. 101, May 2020, doi: 10.3390/membranes10050101.

[89] V. Thomas, T. Bouchez, V. Nicolas, S. Robert, J. F. Loret, and Y. Lévi, “Amoebae in domestic water systems: Resistance to disinfection treatments and implication in Legionella persistence,” J Appl Microbiol, vol. 97, no. 5, pp. 950–963, 2004, doi: 10.1111/j.1365-2672.2004.02391.x.

[90] B. Casini et al., “Detection of viable but non-culturable legionella in hospital water network following monochloramine disinfection,” Journal of Hospital Infection, vol. 98, no. 1, pp. 46–52, Jan. 2018, doi: 10.1016/J.JHIN.2017.09.006.

[91] L. Alleron, N. Merlet, C. Lacombe, and J. Frère, “Long-term survival of Legionella pneumophila in the viable but nonculturable state after monochloramine treatment,” Curr Microbiol, vol. 57, no. 5, pp. 497–502, Nov. 2008, doi: 10.1007/s00284-008-9275-9.

[92] A. B. Molofsky and M. S. Swanson, “Differentiate to thrive: lessons from the Legionella pneumophila life cycle,” Mol Microbiol, vol. 53, no. 1, pp. 29–40, Jun. 2004, doi: 10.1111/j.1365-2958.2004.04129.x.

[93] M. Abdel-Nour, C. Duncan, D. E. Low, and C. Guyard, “Biofilms: The stronghold of Legionella pneumophila,” International Journal of Molecular Sciences, vol. 14, no. 11. pp. 21660–21675, Oct. 31, 2013. doi: 10.3390/ijms141121660.

[94] A. Abu Khweek and A. O. Amer, “Factors mediating environmental biofilm formation by Legionella pneumophila,” Frontiers in Cellular and Infection Microbiology, vol. 8, no. FEB. Frontiers Media S.A., Feb. 27, 2018. doi: 10.3389/fcimb.2018.00038.

[95] M. Campaña, R. del Hoyo, A. Monleón-Getino, and J. Checa, “Predicting Legionella contamination in cooling towers and evaporative condensers from microbiological and physicochemical parameters,” Int J Hyg Environ Health, vol. 248, p. 114117, Mar. 2023, doi: 10.1016/j.ijheh.2023.114117.

[96] L. Conza, S. C. Pagani, and V. Gaia, “Presence of Legionella and Free-Living Amoebae in Composts and Bioaerosols from Composting Facilities,” PLoS One, vol. 8, no. 7, p. e68244, Jul. 2013, doi: 10.1371/journal.pone.0068244.

[97] L. Mueller, H. Traub, N. Jakubowski, D. Drescher, V. I. Baranov, and J. Kneipp, “Trends in single-cell analysis by use of ICP-MS,” Analytical and Bioanalytical Chemistry, vol. 406, no. 27. Springer Verlag, pp. 6963–6977, 2014. doi: 10.1007/s00216-014-8143-7.

[98] L. Rasmussen, H. Shi, W. Liu, and K. B. Shannon, “Quantification of silver nanoparticle interactions with yeast Saccharomyces cerevisiae studied using single-cell ICP-MS,” Anal Bioanal Chem, vol. 414, no. 9, pp. 3077–3086, Apr. 2022, doi: 10.1007/s00216-022-03937-4.

[99] B. Gomez-Gomez, M. Corte-Rodríguez, M. T. Perez-Corona, J. Bettmer, M. Montes-Bayón, and Y. Madrid, “Combined single cell and single particle ICP-TQ-MS analysis to quantitatively evaluate the uptake and biotransformation of tellurium nanoparticles in bacteria,” Anal Chim Acta, vol. 1128, pp. 116–128, Sep. 2020, doi: 10.1016/J.ACA.2020.06.058.

[100] X. Shen et al., “Evaluating the treatment effectiveness of copper-based algaecides on toxic algae Microcystis aeruginosa using single cell-inductively coupled plasma-mass spectrometry,” Anal Bioanal Chem, vol. 411, no. 21, pp. 5531–5543, Aug. 2019, doi: 10.1007/s00216-019-01933-9.

[101] Y. Cao, J. Feng, L. Tang, C. Yu, G. Mo, and B. Deng, “A highly efficient introduction system for single cell- ICP-MS and its application to detection of copper in single human red blood cells,” Talanta, vol. 206, p. 120174, Jan. 2020, doi: 10.1016/J.TALANTA.2019.120174.

[102] S. Y. Lim et al., “Single-cell and bulk ICP–MS investigation of accumulation patterns of Pt-based metallodrugs in cisplatin-sensitive and -resistant cell models,” Metallomics, vol. 14, no. 12, Dec. 2022, doi: 10.1093/mtomcs/mfac085.

VITA

Austin Chase Sigler completed a bachelor's degree in chemistry and human/molecular biology at College of the Ozarks in Point Lookout, Missouri in 2017. Upon completion, he worked as a high school life sciences teacher at Viola Public Schools in Viola, Arkansas. In 2019, Austin joined Honglan Shi's group to pursue doctoral studies in the department of chemistry at Missouri University of Science and Technology. In 2022 Austin accepted a position as a senior scientist for Missouri University of Science and Technology. His doctoral research focused on developing mass spectrometry methods aimed at solving biochemical problems. In May 2023 he received his Ph.D. degree in Chemistry from Missouri University of Science and Technology.